AD-A035 781   ALABAMA UNIV IN HUNTSVILLE   F/G 17/9
A REVIEW OF PULSE COMPRESSION SIGNALS FOR TRACKING APPLICATIONS--ETC(U)
NOV 76   R J POLGE, B K BHAGAVAN   DAAH01-76-C-0991

UNCLASSIFIED   UAH-RR-196   NL

END
DATE
FILMED
3-77

A REVIEW OF PULSE COMPRESSION SIGNALS

FOR

TRACKING APPLICATIONS

by

R. J. Polge
B. K. Bhagavan

FINAL REPORT

VOLUME I

D D C

RECEIVED

FEB 18 1977

D

The University of Alabama in Huntsville
Huntsville, Alabama

November 1976

REPORT DOCUMENTATION PAGE	READ INSTRUCTIONS BEFORE COMPLETING FORM

1. REPORT NUMBER	2. GOVT ACCESSION NO.	3. RECIPIENT'S CATALOG NUMBER
UAH Research Report No. 196		

4. TITLE (and Subtitle)	5. TYPE OF REPORT & PERIOD COVERED
A REVIEW OF PULSE COMPRESSION SIGNALS FOR TRACKING APPLICATIONS. Volume I.	Final Report: Vol. I June - November 1976
	6. PERFORMING ORG. REPORT NUMBER
	UAH Res. Rept. No. 196

7. AUTHOR(s)	8. CONTRACT OR GRANT NUMBER(s)
Robert R. J. Polge B. K. Bhagavan	DAAH01-76-C-0991 new

9. PERFORMING ORGANIZATION NAME AND ADDRESS	10. PROGRAM ELEMENT, PROJECT, TASK AREA & WORK UNIT NUMBERS
The University of Alabama in Huntsville P. O. Box 1247, Huntsville AL 35807	

11. CONTROLLING OFFICE NAME AND ADDRESS	12. REPORT DATE
Hdqts., U. S. Army Missile Command Redstone Arsenal AL 35809 –At: DRSMI-IPBE	November 1976
	13. NUMBER OF PAGES
	79

14. MONITORING AGENCY NAME & ADDRESS(If different from Controlling Office)	15. SECURITY CLASS. (of this report)
UAH-RR-196	Unclassified
	15a. DECLASSIFICATION/DOWNGRADING SCHEDULE

16. DISTRIBUTION STATEMENT (of this Report)

Approved for public release – distribution unlimited 85p.

17. DISTRIBUTION STATEMENT (of the abstract entered in Block 20, If different from Report)

18. SUPPLEMENTARY NOTES

19. KEY WORDS (Continue on reverse side if necessary and identify by block number)

Pulse compression, tracking, binary coding

20. ABSTRACT (Continue on reverse side if necessary and identify by block number)

This report reviews pulse compression signals and their applicability to tracking radars. The emphasis is on binary phase coded signals, such as Barker codes and linear maximal length sequences. The properties of complementary sequences are reviewed and techniques for utilizing these sequences in tracking radars are discussed. Linear frequency modulated signals, polyphase codes and signals with simultaneous amplitude and phase modulation are also considered.

DD FORM 1473 EDITION OF 1 NOV 65 IS OBSOLETE
1 JAN 73

S/N 0102- LF- 014- 6601

389469

A REVIEW OF PULSE COMPRESSION SIGNALS

FOR

TRACKING APPLICATIONS

by

R. J. Polge
B. K. Bhagavan

FINAL REPORT

VOLUME I

D D C

R E C E I V E D

FEB 18 1977

D

The University of Alabama in Huntsville
Huntsville, Alabama

November 1976

PREFACE

This report documents the work performed
by the Communications Group of The University of
Alabama in Huntsville for the U.S. Army Missile
Command on pulse compression signals for tracking
applications, under Contract DAAH01-76-C-0991.

Work continues on the other tasks specified
in the contract and this research will be documented
in subsequent reports.

Robert J. Polge

Huntsville, Alabama

November 1976

ABSTRACT

This report reviews pulse compression signals and their applicability to tracking radars. The emphasis is on binary phase coded signals, such as Barker codes and linear maximal length sequences. The properties of complementary sequences are reviewed and techniques for utilizing these sequences in tracking radars are discussed. Linear frequency modulated signals, polyphase codes and signals with simultaneous amplitude and phase modulation are also considered.

TABLE OF CONTENTS

1. <u>Introduction</u>

Pulse compression involves the transmission of a long coded pulse and the processing of the received echo to obtain a relatively narrow pulse. This technique combines the advantages of high range resolution as in a narrow pulse and of good doppler resolution and high average power as in a wide pulse. Pulse compression is usually achieved by the use of a matched filter whose output, in the absence of doppler shift and noise, is the autocorrelation function of the transmitted signal. Ideally, the autocorrelation must be impulse-like with a large value at zero lag and zero elsewhere, and the degradation due to doppler shift must be small. The presence of secondary peaks, or side lobes, severely limit the performance of the radar. In the case of tracking radars, however, the compressed pulse may be allowed large side lobes provided they fall outside the range bin being tracked. A pulse compression signal is a pulse of finite width with a high bandwidth-time product. For a given pulse width, the bandwidth may be increased by phase and/or amplitude modulation.

The goal of the task reported here is to review and analyze the literature in view of selecting a pulse compression signal for tracking applications of a pulsed radar. The performance criteria are: (i) the peak-to-side lobe ratio of the autocorrelation function, (ii) the distance between the main peak and the first large secondary peak, and (iii) the degradation in the compressed pulse due to small doppler mismatches.

The review of phase modulated signals includes continuous phase modulation and discrete phase modulation. Linear and nonlinear frequency modulations constitute continuous phase modulation. Discrete phase modulation consists of polyphase codes and binary phase codes. Barker codes, shift register generated sequences, and complementary series are the most important binary phase codes that are considered. Huffman codes and generalized Barker codes involve both amplitude and phase modulation. Side lobe reduction may also be affected by processing the matched filter output through a weighting filter. Such filters, suitable for certain types of signals, are also discussed. The final section of the report contains a comparative analysis of the results available in the literature.

2. Signal Modulation and Pulse Compression [5, 10, 14, 47]

In a pulsed radar, the transmitted signal is of the general form,

$$s(t;\omega_0) = \text{rect}_T(t)\ a(t)\ \cos(\omega_0 t - \phi(t)) \tag{2.1}$$

where

$a(t)$ is the amplitude modulation,

$\phi(t)$ is the phase modulation,

$\omega_0 = 2\pi f_0$,

f_0 is the carrier frequency,

$\text{rect}_T(t) = 1$ for $|t| \leq \dfrac{T}{2}$,

$\qquad\qquad = 0$, otherwise,

and T is the width of the pulse.

The return signal from a target at range R and moving with a radial velocity v (range rate) is

$$r(t) = k\ \text{rect}_T(t - \tau)\ a(t - \tau)\ \cos\{(\omega_0 - \omega_d)(t - \tau) - \phi(t - \tau)\}$$

$$= k\ s(t - \tau;\ \omega_0 - \omega_d) \tag{2.2}$$

where $\tau = \dfrac{2R}{c}$ is the delay,

$\omega_d = \dfrac{2v\omega_0}{c}$ is the doppler shift,

k is an attenuation factor,

c is the velocity of propagation,

and v is positive for a target moving away from the radar.

Equation (2.2) is derived using a first order approximation to the round-trip delay due to a varying target range.

The received signal is contaminated by noise generated in the atmosphere or in the antenna and the receiver. Therefore, some form of signal processing is essential prior to detection or target parameter estimation. Assuming white noise, the matched filter is the optimal linear filter which maximizes the signal-to-noise ratio at its output [14, 18, 57]. The impulse response of such a filter is

$$h(t) = s^*(-t; \omega_0 - \omega_d') \tag{2.3}$$

where ω_d' is the selected doppler match and is generally equal to zero. When the doppler shift of the received signal is ω_d', the output of the matched filter $y(t)$ is given by

$$y(t) = k\phi_{ss}(t - \tau) + \phi_{ns}(t - \tau) \tag{2.4}$$

where $\phi_{ss}(\cdot)$ is the autocorrelation of $s(t)$, and $\phi_{ns}(\cdot)$ is the cross-correlation between $n(t)$ and $s(t)$. Assuming that the signal and the noise are sufficiently uncorrelated, $y(t)$ will exhibit a peak at $t = \tau$, which is the desired delay and is a measure of the target range. The peak value is proportional to the energy in the signal and the width of the processed pulse is inversely proportional to the bandwidth of the signal. A doppler mismatch alters the output shape and a two-dimensional correlation function must be introduced. Such a function is the ambiguity function which will be discussed in the next section.

A good range resolution requires that the processed signal be a narrow spike, which can be achieved by using a signal of large bandwidth. One of the means of obtaining a large bandwidth is the reduction in the duration of the pulse. However, since the signal detectability and accuracy of measurements depend on the energy of the signal, the transmitter

power must be raised to keep the energy constant. Peak power limitations and efficient usage of the average power set a lower limit on the pulse duration. The problem, therefore, is to increase the bandwidth of the signal independent of the pulse duration. A monochromatic RF pulse is defined as one whose amplitude and phase modulations, $a(t)$ and $\phi(t)$, are both constant. It can be easily shown that the bandwidth of such a signal is

$$B = \frac{1}{T} \cdot \tag{2.5}$$

Thus the bandwidth can be increased only by reducing the pulse duration, and the time-bandwidth (BT) product is equal to one. In a pulse compression radar, the signal is designed to have a high BT product where a large bandwidth is achieved without sacrificing the pulse duration [4, 7, 31, 47, 52]. This is accomplished by phase modulation, amplitude modulation, or both. In such a situation, the matched filter converts a wide pulse at the input to a narrow pulse at the output and is called the pulse compression filter. Since the width of the input pulse is T and that of the output is $\frac{1}{B}$, the ratio of the input pulse width to the output pulse width is BT. This ratio is also known as the compression ratio.

The most common method for increasing the BT product is phase modulation (PM). The variation of $\phi(t)$ may be continuous as in frequency modulation (linear or nonlinear FM) or discrete (phase-coded signals).

3. Ambiguity Function

The two most important functions of a radar are detection of a target and the estimation of its parameters, such as position and velocity. Target detection is usually performed by subjecting the matched filter (MF) output to a thresholding device. When this output exceeds the threshold, a target is detected and the time at which crossing occurs is a measure of the target range. Because of the presence of noise, detection may occur even in the absence of a target. Therefore, the threshold must be selected to satisfy the specified probability of false alarm. Then, the probability of detection can be increased by increasing the peak value of the MF output which, as mentioned earlier, is proportional to the energy in the pulse.

For a given peak, the accuracy of estimation of the parameters depends upon the shape of the MF output [47]. Assuming no noise interference and zero doppler mismatch, the output is the autocorrelation function of the transmitted pulse. Figure 3.1 shows the autocorrelation functions of three types of radar signals, where the last two include side lobes in addition to the main lobe. If the MF output in Figure 3.1a is passed through a thresholding device, the signal exceeds the threshold for a large period of time. Since the target range is estimated from the time instant at which the threshold is crossed, the spread of the response introduces an uncertainty or ambiguity as to the exact target range. The degree of ambiguity is smaller if the main lobe is narrow. Further, if there are two targets whose range separation corresponds to a delay which is less than the width of the main
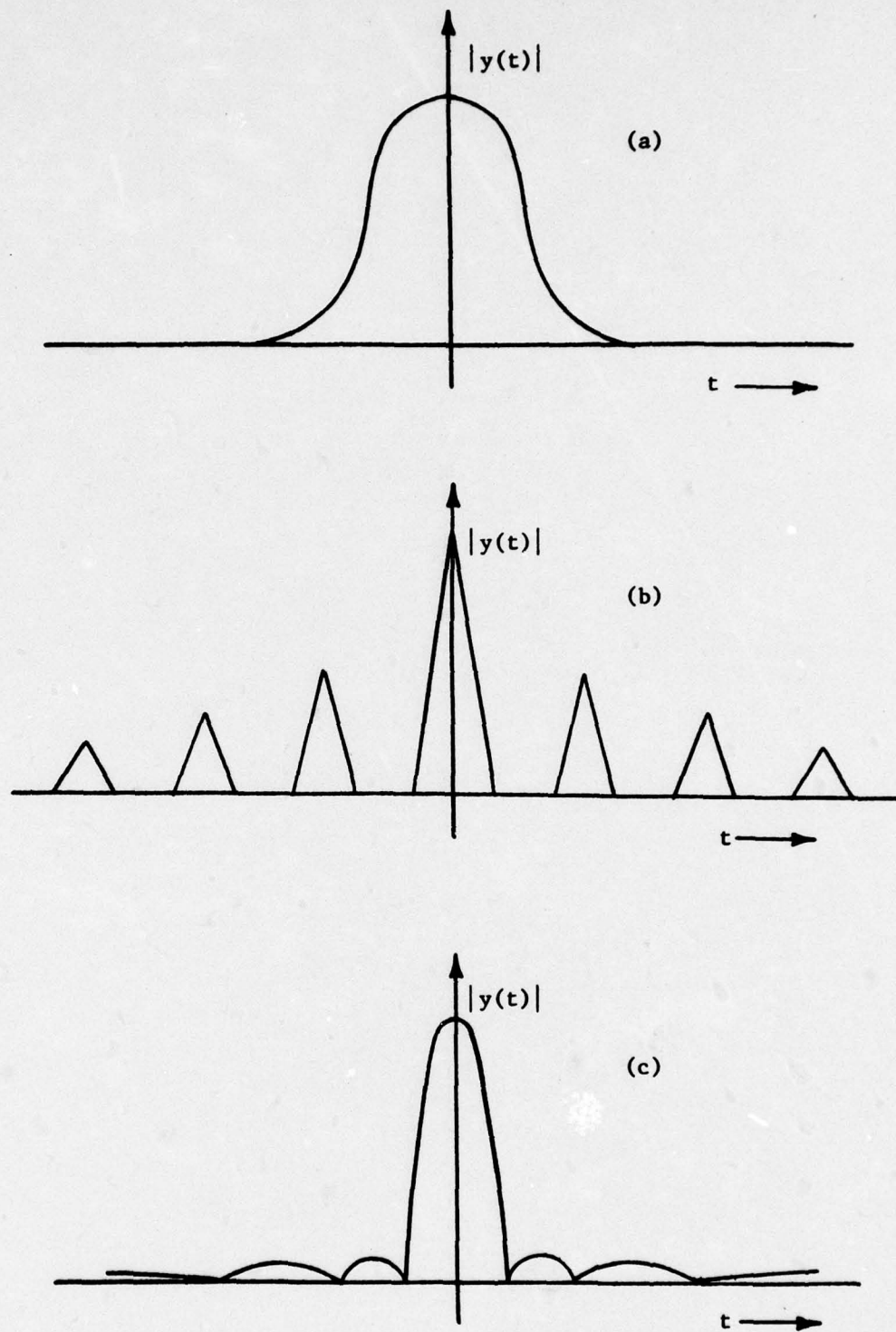
Figure 3.1 Autocorrelations of Three Types of Signals

lobe, it is impossible to resolve the two targets. Figure 3.1b shows a response where the main lobe is narrow enough for the desired separability. However, because of the high side lobes which may also exceed the threshold, the target may be at any one of several ranges. It may also not be possible to distinguish the return due to a single target from a superposition of returns due to several targets. An ideal waveform would be one whose autocorrelation function has one high narrow peak and is zero elsewhere. Such waveforms cannot be realized in practice and, besides, the presence of noise rules out the feasibility of an ideal response. A more practical response is depicted in Figure 3.1c which features a narrow peak and a long tail of side lobes. Here again, a weak target in the vicinity of a strong target will be masked out by the side lobes. Therefore, for a given value for the peak, the desired autocorrelation should have a narrow main lobe and small side lobes.

Thus far, the discussion assumes that there was no doppler mismatch. However, since the target range rate is not known exactly, the matching signal will have a different doppler shift compared to the target return. This could result not only in the reduction of the peak value but also in a time shift, thus promoting inaccuracies in the measurements. Therefore, a two-dimensional autocorrelation function called ambiguity function must be defined for waveform evaluation in terms of ambiguity, resolution, and doppler mismatch.

Before defining the ambiguity function, it is useful to consider the complex representation of radar signals. The transmitted signal

s(t) given in Equation (2.1) can be written as [5, 10, 14, 51]

$$s(t;\omega_0) = \text{Re}\{\psi(t)\} \tag{3.1}$$

where Re $\{\cdot\}$ denotes "real part of" and $\psi(t)$ is a complex signal given by

$$\psi(t) = u(t)\, e^{j\omega_0 t} \tag{3.2}$$

$$\text{and } u(t) = a(t)\, e^{-j\phi(t)} \tag{3.3}$$

Similarly, assuming zero delay, the target return r(t) can be written as

$$r(t) = \text{Re}\{\Lambda(t)\} \tag{3.4}$$

$$\Lambda(t) = v(t)\, e^{j\omega_0 t} \tag{3.5}$$

$$\text{and } v(t) = ka(t)\, e^{-j\phi(t)}\, e^{-j\omega_d t} \tag{3.6}$$

$$= ku(t)\, e^{-j\omega_d t} \ . \tag{3.7}$$

The analysis could be carried out either with the real signals s(t) and r(t) or equivalently, with the corresponding complex signals u(t) and v(t). Assuming that the filter is matched to the signal with zero doppler, the impulse response of the filter is [57]

$$h(t) = u^*(-t) \ . \tag{3.8}$$

The output of the matched filter is

$$w(\tau) = v(\tau) * h(\tau)$$

$$= k \int u(t)\, u^*(t - \tau)\, e^{-j\omega_d t}\, dt \ . \tag{3.9}$$

A two-dimensional correlation function $\chi(\tau,\omega_d)$ is introduced, defined as

$$X(\tau,\omega_d) = \int u(t)\, u^*(t-\tau)\, e^{j\omega_d t}\, dt \; . \tag{3.10}$$

The filter response is easily seen to be

$$w(\tau) = kX(\tau,-\omega_d) \tag{3.11}$$

and the real response of the matched filter is

$$\text{Re}\{kX(\tau,-\omega_d)\, e^{j\omega_0\tau}\} \; .$$

The two-dimensional function $|X(\tau,\omega_d)|$ is known as the uncertainty function and $|X(\tau,\omega_d)|^2$ is called the ambiguity function [47, 64]. The ambiguity function shows the performance of the signal with respect to ambiguity, resolution and the effect of doppler shift. Throughout this analysis, it was assumed that the matching signal had zero doppler. However, if the filter is matched to a doppler of ω_d', then the variable ω_d in the ambiguity function represents the difference between ω_d' and the actual doppler shift. Some of the important properties of the ambiguity function are given below without proof [5, 47].

(a) If $U(\omega)$ is the Fourier transform of $u(t)$, then an alternate expression for $X(\tau,\omega_d)$ would be

$$X(\tau,\omega_d) = \frac{1}{2\pi}\int U^*(\omega)U(\omega-\omega_d)\, e^{j\omega\tau}d\omega \; . \tag{3.12}$$

(b) The ambiguity surface is symmetrical with respect to the origin; i.e.,

$$|X(-\tau,\,-\omega_d)|^2 = |X(\tau,\omega_d)|^2 \; . \tag{3.13}$$

(c) The value at the origin is proportional to the square of the signal energy,

$$|X(0,0)|^2 = \left[\int |u(t)|^2 dt\right]^2$$

$$= 4(\text{signal energy})^2 \qquad (3.14)$$

(d) The absolute maximum value of the ambiguity surface is at the origin; thus

$$|X(\tau,\omega_d)|^2 \leq |X(0,0)|^2 . \qquad (3.15)$$

(e) The total volume under the ambiguity surface is

$$\iint |X(\tau,\omega_d)|^2 d\tau \ d\omega_d = 2\pi |X(0,0)|^2 . \qquad (3.16)$$

The above equation states that the total volume is a function only of the signal energy, and whatever is done to make $|X(\tau,\omega_d)|^2$ small in one part of the τ,ω_d plane will result in an increase somewhere else. Thus, if one chooses a signal whose ambiguity has a narrow central spike, the bulk of the volume must appear as side lobes, possibly masking targets which are relatively far away. If it is important to avoid such masking, the volume must be concentrated about the origin, resulting in a broad central peak with its inherent disadvantages.

The matched filter receiver is optimized for signal detection in white noise, but may have the disadvantage of relatively high side lobes. In this case, a weighting filter is used in conjunction with the matched filter to reduce the side lobes [14, 51]. Such a deliberate mismatch inevitably degrades noise performance, but it is conceivable that a good compromise can be found between improvement in resolution and deterioration in detection performance. The most common reason for mismatching is the suppression of range side lobes. Specifically, the

heights of the side lobes are reduced at the cost of widening and reducing the main lobe.

In the application being considered in this study, the radar is assumed to be in the tracking mode and, therefore, good estimates of the range and the range rate are available. Thus only the matched filter output corresponding to a few range cells around the estimated range are considered, the rest of it being essentially ignored. Large side lobes can therefore be allowed to exist outside this interval of interest. This means that only a small portion of the ambiguity surface around the origin needs to be examined while evaluating the performance of a given waveform.

4. Linear and Nonlinear FM

The instantaneous frequency of the complex envelope $u(t)$ is defined as

$$f_i(t) = \frac{-1}{2\pi} \frac{d\phi(t)}{dt} \quad . \tag{4.1}$$

PM waveforms for which the phase $\phi(t)$ is nonlinear but where it is convenient to express the modulation of the instantaneous frequency are called FM waveforms. Linear FM [32, 37, 44] is defined by an instantaneous frequency which is a linear function of time,

$$f_i(t) = \frac{1}{2\pi} \mu t \quad \text{for } \frac{-T}{2} \le t \le \frac{T}{2} \tag{4.2}$$

and a corresponding phase modulation,

$$\phi(t) = \frac{-1}{2} \mu t^2 \quad . \tag{4.3}$$

The complex modulation function $u(t)$ is given by

$$u(t) = e^{j\mu t^2/2} \quad . \tag{4.4}$$

The frequency sweep of this signal is $-\frac{B}{2}$ to $\frac{B}{2}$, where the bandwidth B is

$$B = \frac{\mu T}{2\pi} \quad . \tag{4.5}$$

It can be easily shown that the uncertainty function of this waveform is [5, 14, 20]

$$\left| X(\tau, \omega_d) \right| = \left| \frac{\sin\left(\frac{\mu\tau - \omega_d}{2}\right) T \left(1 - \frac{|\tau|}{T}\right)}{\frac{\mu\tau - \omega_d}{2}} \right| \tag{4.6}$$

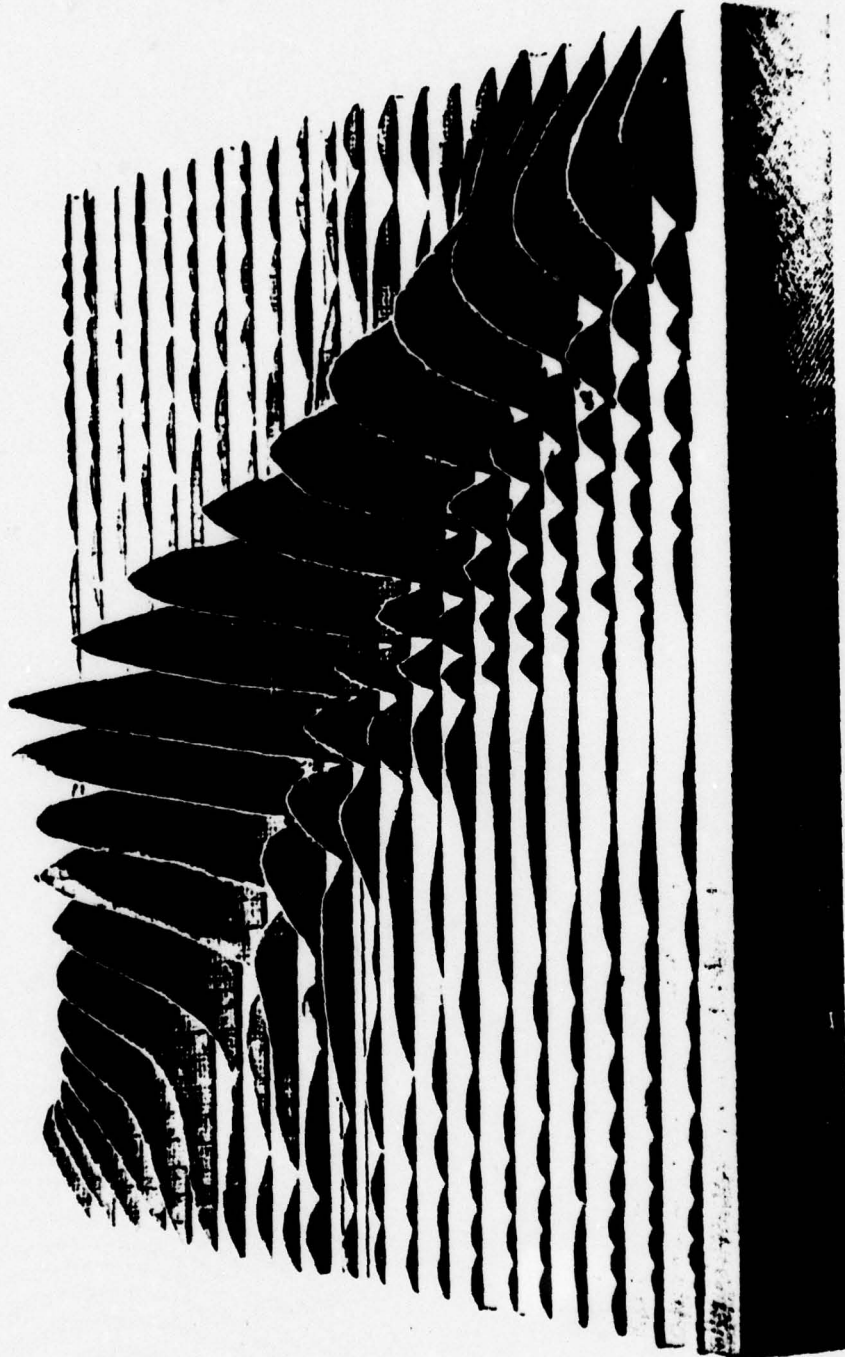and is depicted in Figure 4.1. For small values of τ, ignoring the

Figure 4.1   Uncertainty Function of a Linear FM Signal, BT = 10
(Reproduced from [20])

relatively slowly varying factor $\left(1 - \frac{|\tau|}{T}\right)$, the function $|X(\tau, \omega_d)|$ can be approximated as

$$|X(\tau, \omega_d)| \cong T \left| Sa\left\{ \frac{T}{2} (\mu\tau - \omega_d) \right\} \right| \qquad (4.7)$$

where $Sa(x) = \frac{\sin x}{x}$.

Thus, any cut parallel to the delay or doppler axis yields a $|Sa(x)|$ function, with the peak occurring at

$$\mu\tau - \omega_d = 0$$

or

$$\tau = \frac{\omega_d}{\mu} \quad . \qquad (4.8)$$

In other words, a doppler mismatch of ω_d results in an equivalent time delay of $\frac{\omega_d}{\mu}$, thus reducing the accuracy of the range measurement. The factor $\left(1 - \frac{|t|}{T}\right)$ decreases the amplitude as one moves away from the doppler axis. Thus a doppler mismatch results in a reduction of the peak and delays it by an amount proportional to the mismatch. In the vicinity of the origin, the response along the delay axis can be approximated as

$$Sa\left(\frac{\mu T \tau}{2}\right) = \frac{\sin (\mu T \tau/2)}{(\mu T \tau/2)}$$

$$= \frac{\sin \pi B \tau}{\pi B \tau} \quad . \qquad (4.9)$$

The half power width of the central peak is of the order of (1/B). Since the input pulse width is T, the compression factor is BT, the time-bandwidth product. Similarly, it can be shown that the half power width in doppler is about (1/T). The autocorrelation structure described by

(4.9) also indicates the existence of severe side lobes. In fact, the height of the first side lobe is within -13.5 dB of the central peak.

Two drawbacks of linear FM are: (1) the range-doppler coupling as suggested by (4.8), and (2) the existence of relatively large range side lobes. In many applications, a good estimate of the doppler is available, and the range estimate can be corrected to account for doppler mismatch. Otherwise, it is necessary to use an entire bank of filters, each matched to a particular value of doppler. This, of course, is also necessary if a doppler measurement is contemplated.

The range side lobes can be suppressed using weighting filters [14, 55, 63], thus creating an intentional mismatch. As mentioned earlier, weighting filters achieve side lobe suppresion at the cost of reduced resolution and signal detectability. The loss in resolution is a result of broadening of the main lobe and the reduction in the central peak (hence, the signal-to-noise ratio) causes the loss in detectability. The Dolph-Chebyshev weighting [14] is optimum in the sense that it has the smallest main lobe expansion for a specified side lobe suppression. However, it is not physically realizable and several approximations to it have been suggested. The most important among these are the Taylor approximation, Hamming weighting, and the general cosine-power weighting. A sixth order Taylor weighting designed for a peak side lobe level of -40 dB also results in a main lobe widening by a factor of 1.41 and in a loss in the signal-to-noise ratio of 1.2dB. The Hamming weighting is considerably less difficult to realize than the Taylor weighting and is a particular case of a cosine-squared function on

a baseline pedestal. The performance figures for Hamming weighting are: peak side lobe level of -42.8 dB, main lobe widening factor of 1.47, and loss in signal-to-noise ratio of 1.34 dB. Reduced side lobes can also be achieved by amplitude weighting or amplitude modulation of the transmitted signal.

The strong coupling between range and range rate can be attributed to substantial match in the instantaneous frequencies of a delayed, doppler-shifted signal and that of the matching signal as seen in Figure 4.2.
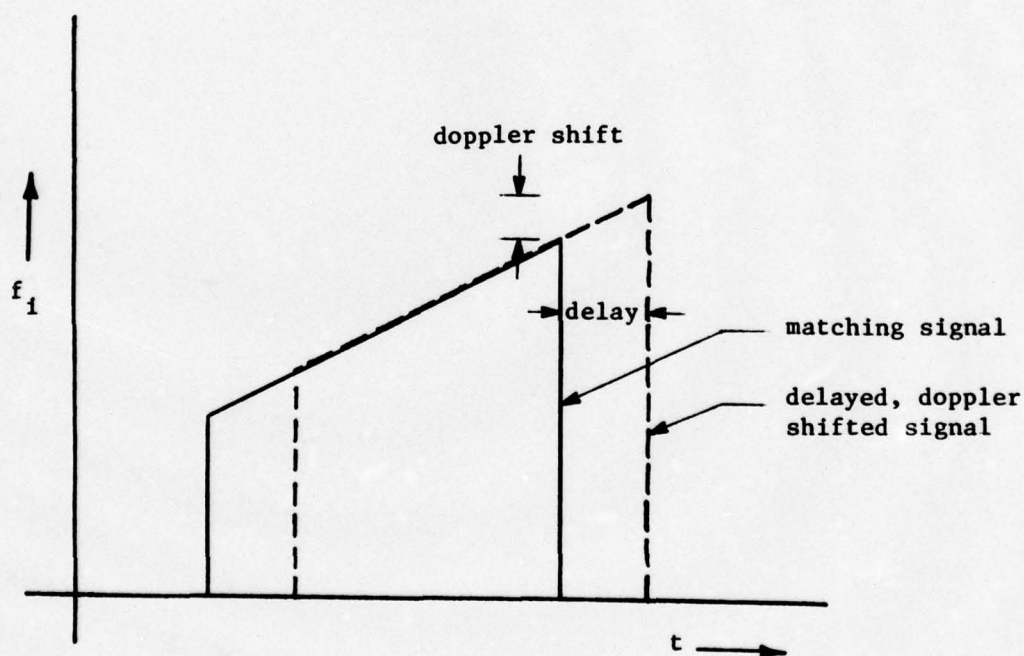
Figure 4.2   Instantaneous Frequency of Linear FM Signal

One possible method of lessening this match is the use of nonlinear modulation such as quadratic FM and piecewise linear FM [47]. Even though the peaks due to range-doppler coupling are reduced, high ridges appear elsewhere because the volume under the ambiguity surface is constant.

5. Polyphase Codes [21, 27, 40, 41, 51]

The previous section was concerned with continuous frequency (or phase) modulation. In this and the following sections, a class of signals called the phase coded signals will be discussed. These waveforms feature ordered sequences that are impressed, at fixed time intervals, on the phase of the carrier. In other words, the phase modulation $\phi(t)$ is assumed to be piecewise constant,

$$\phi(t) = \phi_n \quad \text{for } (n - 1)\delta \leq t \leq n\delta , \quad n = 1, 2, \cdots, N \qquad (5.1)$$

where $T = N\delta$. $\qquad\qquad\qquad\qquad\qquad\qquad\qquad\qquad\qquad\qquad\qquad\qquad$ (5.2)

Polyphase codes with zero periodic correlation except at zero shift were developed by Heimiller [27]. These codes are of length $N = p^2$ where p is a prime number and p different phases corresponding to the pth roots of unity are required to generate the codes. The restriction that p be prime was later removed by Frank and Zadoff [22]. Frank [21] described a method for generating non-periodic polyphase codes using the same construction as for periodic codes. The code of length $N = p^2$ is described by a p x p matrix:

$$
\begin{matrix}
0 & 0 & 0 & 0 & \cdots & 0 \\
0 & 1 & 2 & 3 & \cdots & (p-1) \\
0 & 2 & 4 & 6 & \cdots & 2(p-1) \\
0 & 3 & 6 & 9 & \cdots & 3(p-1) \\
\cdot & & & & & \\
\cdot & & & & & \\
\cdot & & & & & \\
\cdot & & & & & \\
0 & (p-1) & (2(p-1) & \cdots & & (p-1)^2 \quad .
\end{matrix}
\qquad (5.3)
$$

The elements represent multiplying coefficients of a basic phase angle ($2\pi k/p$) where k is an integer and is relatively prime to p (k is usually equal to 1). The non-periodic sequence is obtained by placing the rows side by side, yielding a sequence containing p^2 elements. For example, let p = 4; then the matrix is

$$
\begin{array}{cccc}
0 & 0 & 0 & 0 \\
0 & 1 & 2 & 3 \\
0 & 2 & 4 & 6 \\
0 & 3 & 6 & 9
\end{array}
\tag{5.4}
$$

and the basic phase angle is

$$
\theta = \frac{2\pi}{p} = \frac{\pi}{2} \quad . \tag{5.5}
$$

The sequence of phases $\{\phi_n, \ n = 1, 2, \ \cdots, 16\}$ can be written as

$$\{0, \ 0, \ 0, \ 0, \ 0, \ \theta, \ 2\theta, \ 3\theta, \ 0, \ 2\theta, \ 4\theta, \ 6\theta, \ 0, \ 3\theta, \ 6\theta, \ 9\theta\} \ .$$

As mentioned before, the codes were originally designed to give zero periodic correlation, and this optimum side lobe performance is not obtained with non-periodic correlation. Cyclic shifting of the codes given above results in new codes with different non-periodic autocorrelation structures. But it has been found that the sequence as given above possesses the most desirable structure.

The phase variation of the Frank polyphase code can be considered as a piecewise constant approximation to a parabola; thus the Frank polyphase code is an approximation to linear FM.

Frank has conjectured that the maximum side lobe is the vector sum of p/2 (for p even) or (p + 1)/2 (for p odd) unit vectors where the

vectors are separated by $2\pi/p$. This implies that for large p, the peak
side lobe amplitude approaches p/π and the peak-to-side lobe ratio
approaches πp [14]. The actual ratios for values of p from 3 to 8 are
given in Table 5.1.

TABLE 5.1 Peak-to-Side Lobe Ratios for Polyphase Codes

p	N	Peak Side Lobe Amplitude	Peak-to-Side Lobe Ratio (dB)
3	9	1.0	19.08
4	16	1.4	21.16
5	25	1.6	23.88
6	36	2.0	25.11
7	49	2.25	26.76
8	64	2.6	27.82

Matched filter outputs for doppler shifted polyphase codes of
length N = 100 are shown in Figures 5.1(a) - 5.1(g) for different
values of doppler shifts [14]. It can be seen from these figures that
the polyphase codes have doppler degradations somewhat similar to those
of linear FM. The main peak shifts its position as a function of
doppler shift and its value decreases as the doppler shift increases.
In addition, there are secondary peaks which are cyclic as functions
of doppler shift. At higher dopplers, an image signal also develops
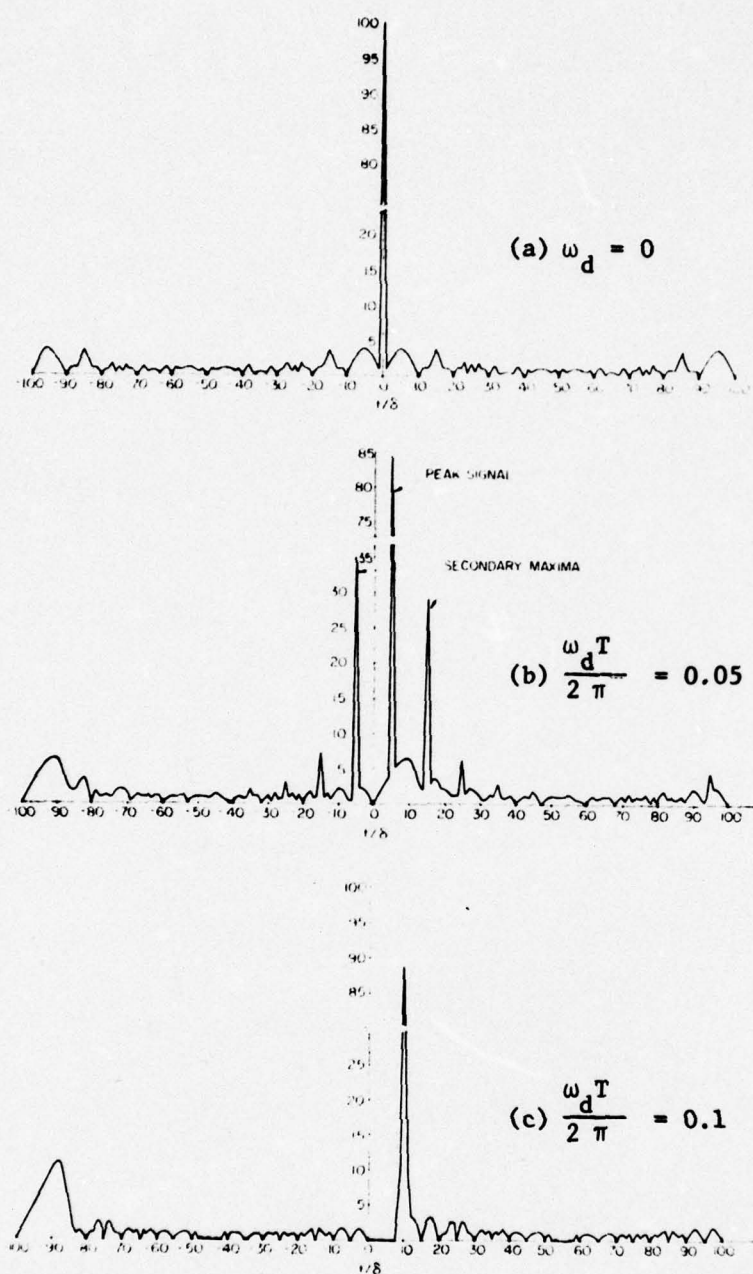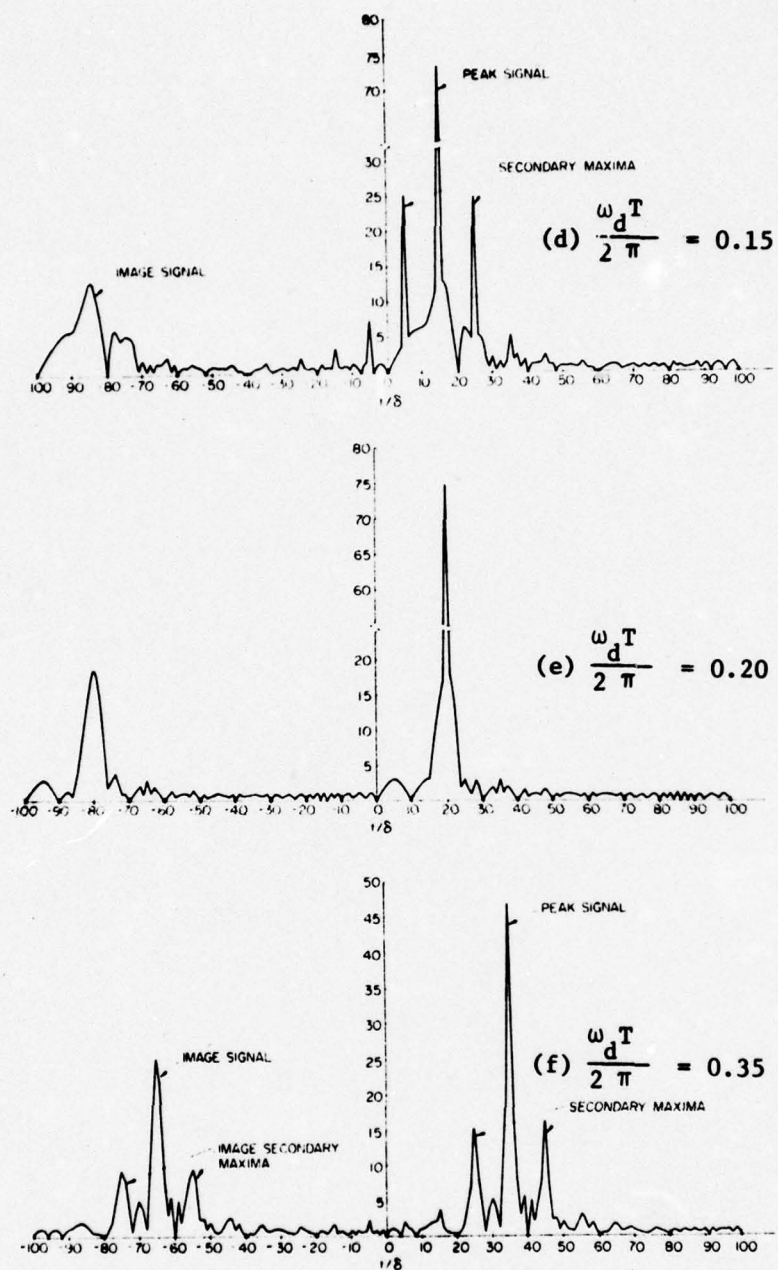so that the output breaks up into two similar signals.

Figure 5.1   Matched Filter Outputs for Polyphase Codes
with Different Doppler Mismatches

Figure 5.1   Matched Filter Outputs for Polyphase Codes
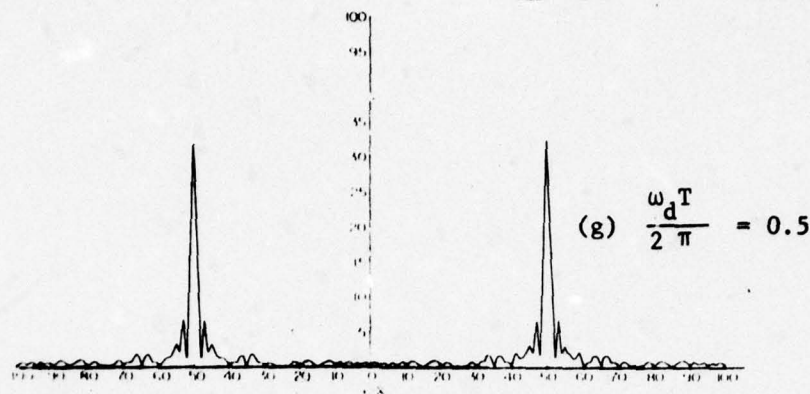with different doppler mismatches

(g) $\dfrac{\omega_d T}{2\pi} = 0.5$

Figure 5.1   Matched Filter Outputs for Polyphase Codes
with Different Doppler Mismatches

Other three-phase codes consisting only of the cube roots of unity
were investigated by DeLong [16].   Existence of such sequences has not been
established for lengths greater than 9. Four-phase codes have also been
considered because of their simplicity of implementation.   Four-phase approxi-
mations to Frank codes of length greater than 16 and to linear FM have been
studied.

Sequences constructed from two or more phases and possessing the
property that the magnitude of the autocorrelation at any non-zero delay is
less than one were investigated by Golomb and Scholtz [26].   Such sequences
are called Generalized Barker Sequences, and a four-phase sequence of length
15 has been described.   Also included in this paper is an exhaustive tabu-
lation of six-phase sequences of lengths N = 3 to N = 12.   Existence of
longer sequences has not been established even though there appear to be
no theoretical constraints which would preclude them.

Codes which involve amplitude modulation in addition to phase modu-
lation have also been investigated.   Some of these codes, such as Huffman
codes and ternary sequences, will be described in Section 9.   When

the number of distinct phases involved in a polyphase code is 2, the

code reduces to a binary phase code. Because of the extensive research

performed on binary codes, they are treated separately in the following

sections.

6. Barker Codes

The simplest form of phase coding is the binary or phase-reversal code in which the phase ϕ_n is either zero or 180°. The complex representation of such a signal is given by,

$$\psi(t) = u(t)\, e^{j\omega_0 t} \tag{6.1}$$

where

$$u(t) = e^{-j\phi_n} \quad \text{for } (n-1)\delta \le t \le n\delta \tag{6.2}$$

$$\phi_n = 0 \text{ or } 180° \tag{6.3}$$

$$\left.\right\} \quad n = 1, 2, \cdots, N$$

and

$$T = N\delta . \tag{6.4}$$

Combination of (6.2) and (6.3) yields

$$u(t) = \sum_{n=1}^{N} a_n R_n(t) \tag{6.5}$$

where $R_n(t) = 1$ for $(n-1)\delta \le t \le n\delta$

$$= 0 \text{ elsewhere} \tag{6.6}$$

and

$$a_n = \pm 1 . \tag{6.7}$$

It can be easily shown that the autocorrelation of such a waveform is made up of triangular pulses, and hence $\chi(\tau,0)$ may be obtained by calculating the function $\chi(k\delta,0)$ for integral values of k and combining these points by straight lines. The discrete samples of the autocorrelation are given by

$$\chi(k\delta,0) = \sum_{n=1}^{N-1-|k|} a_n a_{n+|k|} . \tag{6.8}$$

The Barker codes or Barker sequences are a family of binary sequences characterized by [5, 14, 15, 43, 51, 59]

$$X(k\delta,0) = N \qquad \text{for } k = 0$$

$$= 0, \pm 1 \quad \text{for } k \neq 0 \ . \tag{6.9}$$

Because of this desirable property, they are also called **perfect words** and **optimal sequences**. The size of this family of codes is restricted; in fact, Barker sequences are known to exist only for seven lengths. These are given in Table 6.1, where + and − represent +1 and −1, respectively.

TABLE 6.1   BARKER SEQUENCES

LENGTH N	
2	+ +
2	+ −
3	+ + −
4	+ + − +
4	+ + + −
5	+ + + − +
7	+ + + − − + −
11	+ + + − − − + − − + −
13	+ + + + + − − + + − + − +

It has been proved that Barker sequences do not exist for odd lengths greater than 13 and that the existence of even length Barker code requires that N be a perfect square [39, 53, 58, 59]. Further, it has been shown that no even length Barker sequences exist for N < 6084 [58].

Figure 6.1 shows the magnitudes of the matched filter outputs for different values of doppler mismatch. The figure shows slices at doppler intervals of $(2\pi/4T)$, with the zero doppler slice in the front. As can be easily seen, the response deteriorates rapidly for large values of doppler mismatch. Because of the high peaks exhibited at non-zero dopplers, these codes are not desirable even if a bank of matched filters is used for all possible dopplers.

Even for the longest available Barker code (N = 13), the peak side lobe at zero doppler mismatch is only 22.3 dB below the main peak. In a multi-target environment, such high side lobes are undesirable. As in the case of linear FM, one way to suppress the side lobes is in the use of a weighting filter. The geometric similarity between the main lobe and the side lobes (they are triangles of equal width) is used to synthesize a weighting filter using delay lines. Figure 6.2(a) shows the autocorrelation function $\rho(t)$ of the Barker sequence of length 13. Each of the side lobes can be independently reduced to any desired level by adding weighted and delayed replicas of the function itself [20, 38]. Consider a 2K + 1 order network with impulse response,

$$h(t) = \sum_{k=-K}^{K} \beta_k \delta(t - 2k\delta) \tag{6.10}$$

where $\delta(\cdot)$ is the Dirac delta function. If the input to this filter is $\rho(t)$, then it can be easily shown that its output is given by

$$g(t) = \sum_{k=-K}^{K} \beta_k \rho(t - 2\delta) . \tag{6.11}$$
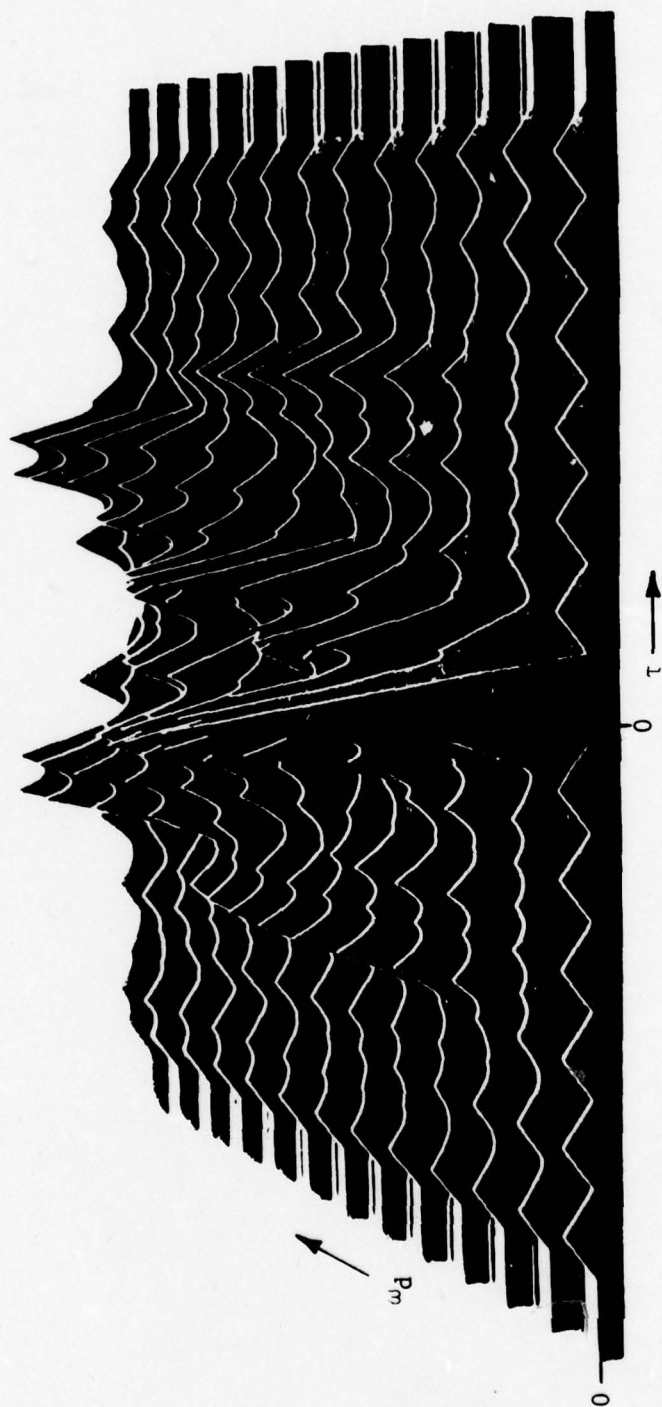
Figure 6.1   Uncertainty Function for the 13-bit Barker Code
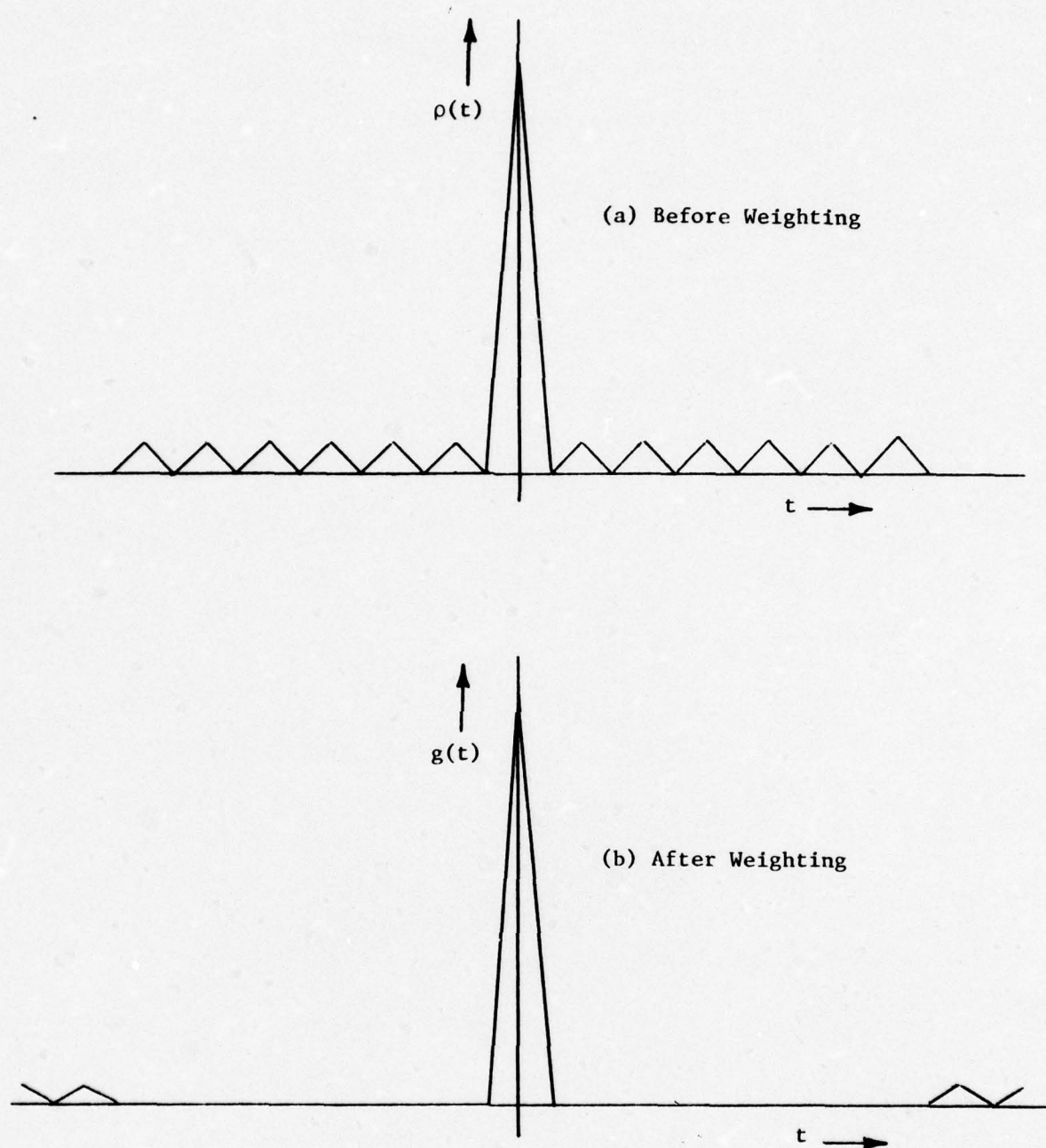(Reproduced from [20])

Figure 6.2   Barker Code Autocorrelation Before and
After Weighting

It is desirable to maintain the evenness of the response; thus,

$$\beta_k = \beta_{-k} \ . \tag{6.12}$$

It is now required to choose $K + 1$ weighting factors β_0, β_1, $\cdots$, β_K to provide the desired side lobe suppression. One possible criterion is to reduce the first K side lobes to zero while maintaining a value of 13 for the main lobe. For example, if $N = 13$ and $K = 6$, this criterion results in 7 linear equations in the seven unknown wieghting factors. Solution of these equations yields the following values:

$$\beta_0 = 1.047722 \ , \quad \beta_1 = -0.040733 \ , \quad \beta_2 = -0.045572 \ , \quad \beta_3 = -0.050094$$
$$\beta_4 = -0.054269 \ , \quad \beta_5 = -0.058066 \ , \quad \beta_6 = -0.061461 \quad .$$

The weighting filter can be easily mechanized with a delay line network as shown in Figure 6.3. The output of the filter $g(t)$ is shown in Figure 6.2(b). As can be seen, the first six side lobes have been completely suppressed but the weighting filter has introduced additional side lobes at delays larger than 13δ. The main lobe-to-side lobe ratio of this signal is about 32.4 dB, an improvement of 10 dB over the non-weighted signal. More important, the side lobes at smaller delays are completely cancelled, making it attractive for tracking applications. A 25th order network designed to suppress the first 12 side lobes yields a main lobe-to-side lobe ratio of 45 dB. As mentioned earlier, the use of a weighting filter destroys the optimality of the matched filter, resulting in a loss in detection capability (signal-to-noise ratio). It has been shown that the maximum loss for the Barker code of length 13 is 0.25 dB.

Weighting filters can also be designed in the frequency domain [46]. The Fourier transform of the autocorrelation function $\rho(t)$ can be shown to be
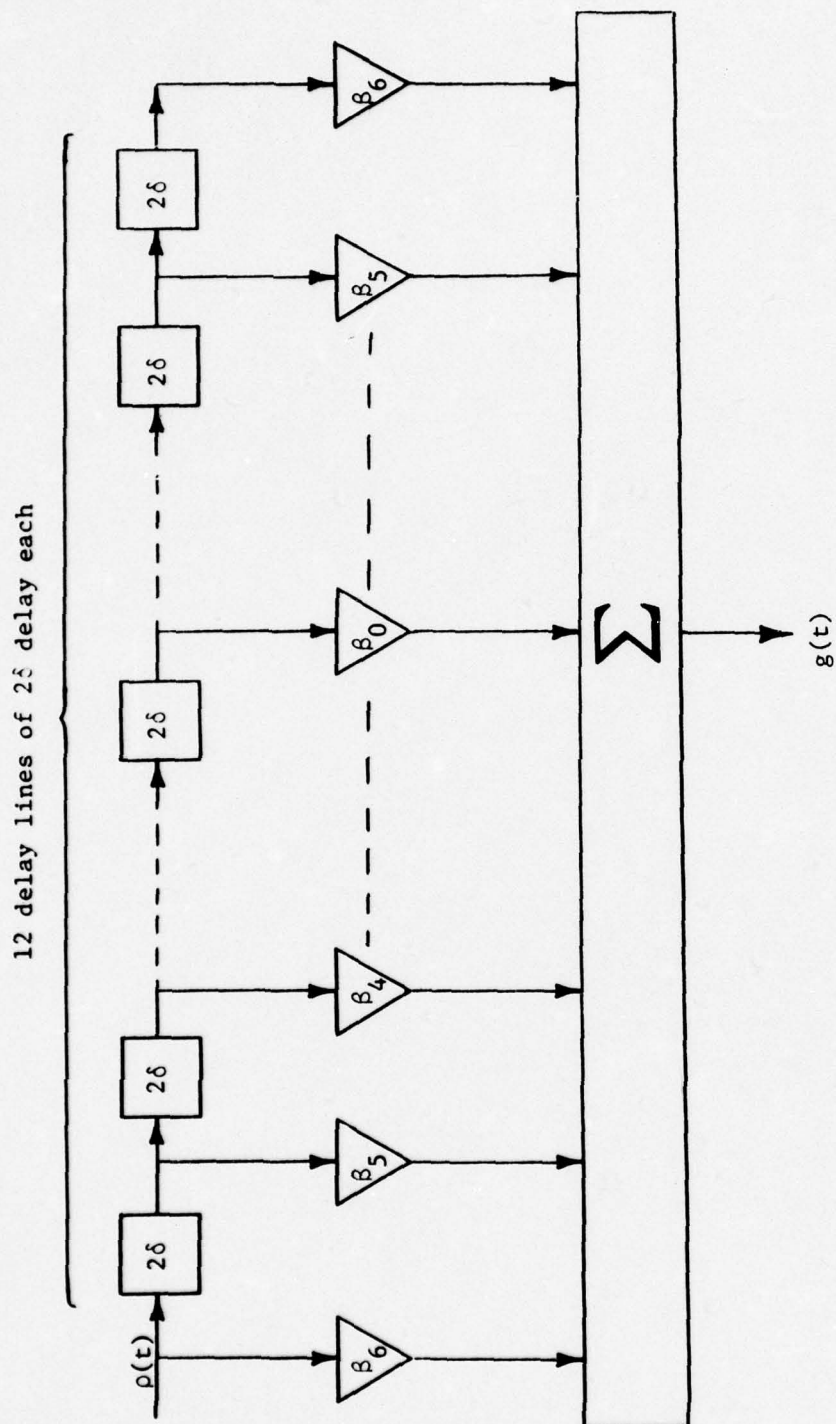
12 delay lines of 2δ delay each

Figure 6.3 The Weighting Network

$$P(\omega) = \delta \; Sa^2(\omega\delta/2) \left[12 + \frac{\sin 13 \; \omega\delta}{\sin \omega\delta} \right] . \tag{6.13}$$

The transform of the desired portion (the main lobe) is

$$G(\omega) = 13\delta \; Sa^2(\omega\delta/2) . \tag{6.14}$$

Thus the desired signal can be extracted by inverse filtering; i.e., by passing $\rho(t)$ through a filter whose transfer function is

$$H(\omega) = G(\omega)/P(\omega)$$

$$= \frac{13}{12 + \dfrac{\sin 13 \; \omega\delta}{\sin \omega\delta}} . \tag{6.15}$$

Weighting filters have been designed to approximate this transfer function. Delay line filters based on this approximation can be obtained from a truncated Fourier series expansion of $H(\omega)$. Other approximations including the use of feedback structures have also been investigated.

Although one can suppress the side lobes of Barker codes, these codes allow only low pulse compression factors because of the limited length. Longer codes can be achieved by phase coding within each segment of one Barker code with another Barker code. Such sequences have been called combined Barker sequences, multistage Barker codes, or Barker squared codes [29, 30]. Each pulse of the new code may in turn be replaced by an entire code, and so forth. By using relatively short codes of lengths N_1, N_2, N_3, $\cdots$, one obtains a large overall code length of $N_1 N_2 N_3 \cdots$. Figure 6.4 shows the autocorrelation function of the Barker code of length 13 where each segment is coded with a Barker code of length 4. When the roles of the codes of length 13 and 4 are reversed, the resulting autocorrelation is as shown in Figure 6.3. In either case, a compression ratio of 52 has been achieved, but the side lobes are considerably stronger than those of a Barker code.
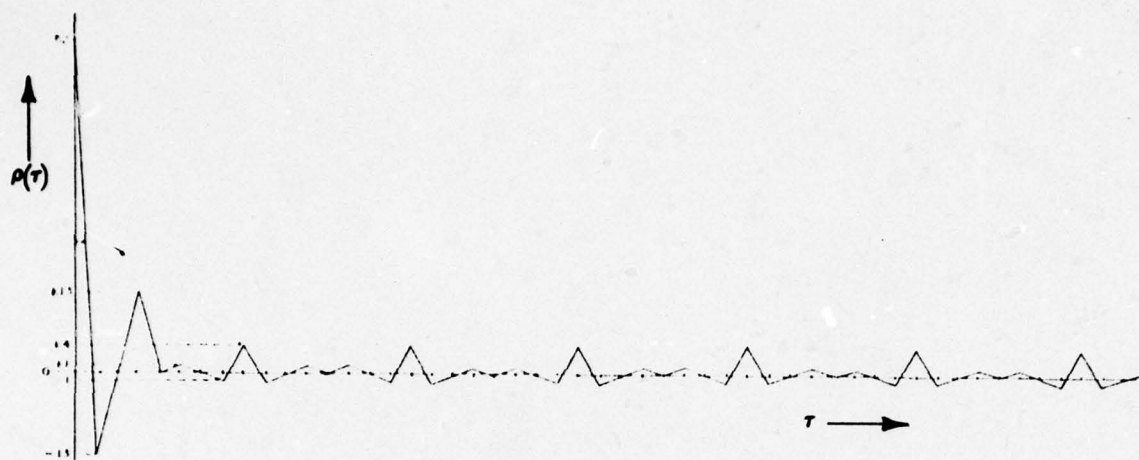
Figure 6.4   Autocorrelation of a 13-bit Barker Code each bit of
which is a 4-bit Barker Code

Figure 6.5   Autocorrelation of a 4-bit Barker Code each bit of
which is a 13-bit Barker Code

Here again, side lobe suppression can be effected by the use of a weighting filter. Either of the two methods mentioned earlier can be used for this purpose. The applicability of the second method can be proved as follows [46]. Consider a Barker code consisting of N_1 pulses of duration δ each. Then, assuming positive side lobes (i.e., $N_1 = 2, 5$ or 13), the autocorrelation of this code is

$$\rho_1(\tau) = (N_1 - 1)d(\tau) + \sum_{n = -(N_1 - 1)/2}^{(N_1 - 1)/2} d(\tau - 2n\delta) \qquad (6.16)$$

where $d(\tau)$ is the autocorrelation of an individual pulse. If this code is repeated in the form of a positive side lobe Barker code of length N_2, the autocorrelation of the new code will be

$$\rho_2(\tau) = (N_2 - 1)\rho_1(\tau) + \sum_{n = -(N_2 - 1)/2}^{(N_2 - 1)/2} \rho_1(\tau - 2n\delta) \quad . \qquad (6.17)$$

By taking the Fourier transforms of $\rho_1(t)$ and $\rho_2(t)$, it can be shown that

$$P_1(\omega) = D(\omega) \left[N_1 - 1 + \frac{\sin N_1 \omega\delta}{\sin \omega\delta} \right]$$

$$= D(\omega) F_1(\omega) \qquad (6.18)$$

and $$P_2(\omega) = P_1(\omega) \left[N_2 - 1 + \frac{\sin N_2 \omega\delta}{\sin \omega\delta} \right]$$

$$= P_1(\omega) F_2(\omega)$$

$$= D(\omega) F_1(\omega) F_2(\omega) \quad . \qquad (6.19)$$

The desired signal $d(\tau)$ can therefore be obtained by passing $\rho_2(\tau)$ through a filter whose transfer function is

$$H(\omega) = \frac{1}{F_1(\omega) F_2(\omega)} \quad .$$

Approximations to this transfer function can be used, as before, to reduce the range side lobes.

7.   Shift Register Generated Sequences
[6, 24, 25, 45, 48]

A shift register sequence generator consists of a shift register working in conjunction with appropriate logic, which feeds back a logical combination of the states of two or more of its stages to its input.   A shift register generator (SRG) of degree n consists of n storage elements (n stages), a clock pulse generator, and a feedback logic circuit as shown in Figure 7.1.   When a clock pulse arrives, the contents of each stage are transferred to the next stage.   The new state of the first stage is an arbitrary Boolean function of the previous contents of the register.   For each stage, the off state is symbolized by 0 and the on state by 1.   The binary output of the feedback logic unit is a Boolean function of n binary inputs, and there are 2^{2^n} different Boolean functions for a given n.   A shift register generated sequence is therefore specified by the particular Boolean function chosen
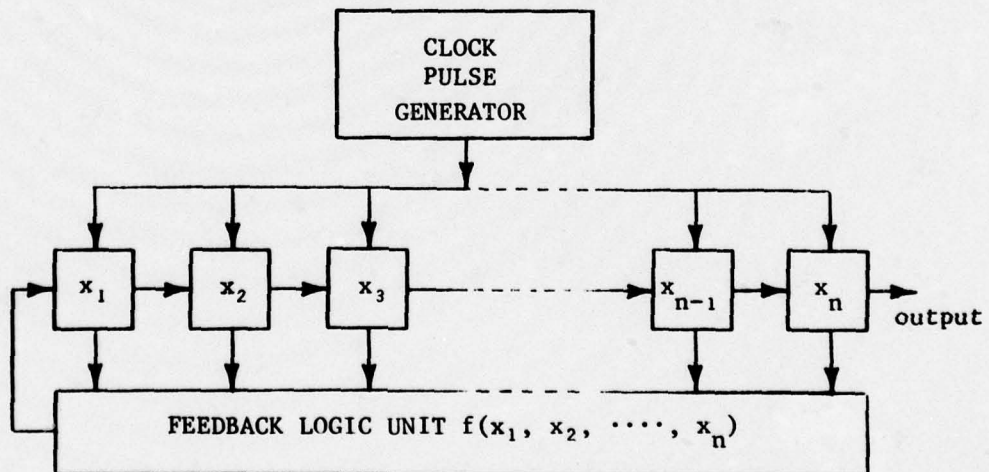
Figure 7.1   The General Shift Register Generator

and the initial state of the register. It can be shown that the output sequence of an n stage generator is periodic with period $p \leq 2^n - 1$ and that for every n, there actually exist feedback arrangements which lead to the maximum period $N = 2^n - 1$. Sequences with the maximum period are called maximum length sequences.

Denote by x_i the state of the ith stage and let $f(x_1, x_2, \cdots, x_n)$ denote the Boolean feedback function. The shift register is called linear if this function can be expressed as

$$f(x_1, x_2, \cdots, x_n) = C_1 x_1 \oplus C_2 x_2 \oplus C_3 x_3 \oplus \cdots \oplus C_n x_n \qquad (7.1)$$

where each constant C_i is either zero or one and where the symbol $\oplus$ denotes addition modulo 2. Otherwise, the shift register is nonlinear. Since there are 2^n ways to pick the n constants C_i, only 2^n of the 2^{2^n} shift registers with n stages are linear. An example of a simple 5-stage linear SRG is whown in Figure 7.2 where

$$C_2 = C_5 = 1 \quad \text{and} \quad C_1 = C_3 = C_4 = 0$$

and
$$f(x_1, x_2, x_3, x_4, x_5) = x_2 \oplus x_5 \qquad (7.2)$$

Linear maximum length (ML) shift register generated sequences or linear m-sequences have been investigated in great detail. It has
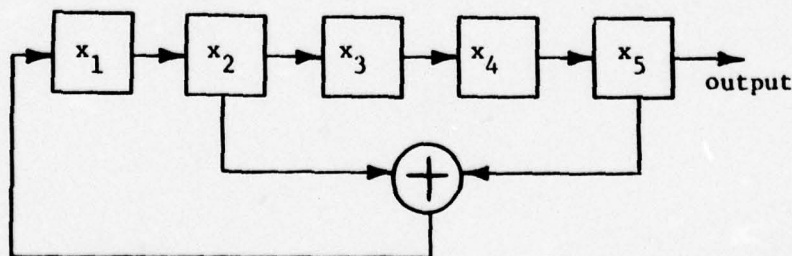

Figure 7.2 Five Stage Linear SRG

been proved that such sequences exist for every register length n. The linear feedback functions which yield m-sequences have been extensively tabulated [9, 17, 65] and a part of it is shown in Table 7.1. The use of this table will be demonstrated with an example. Consider a 5-stage generator, n = 5 for which the maximum period is $N = 2^5 - 1 = 31$. The table lists 3 possible feedback connections:

(i) [5,2] which corresponds to a feedback connection described by

$$f(x_1, x_2, x_3, x_4, x_5) = x_2 \oplus x_5 \qquad (7.3)$$

(ii) [5,4,3,2] which corresponds to

$$f(x_1, x_2, x_3, x_4, x_5) = x_2 \oplus x_3 \oplus x_4 \oplus x_5 \qquad (7.4)$$

and (iii) [5,4,2,1] which corresponds to

$$f(x_1, x_2, x_3, x_4, x_5) = x_1 \oplus x_2 \oplus x_4 \oplus x_5 \qquad (7.5)$$

Figure 7.2 shows the feedback connections for the first of these generators. In addition to the connections listed in the table, there exist other combinations which produce sequences which are mirror images of those obtained using the table. For example, if the table shows the connection

$$[n, t_1, t_2, t_3 \cdots] ,$$

the mirror image sequence is obtained from the connection

$$[n, n-t_1, n-t_2, n-t_3, \cdots] .$$

It should be noted, too, that for a given connection, different initial conditions produce the same sequence with different shifts. The output of the shift register generator is a sequence of zeros and ones. The

Table 7.1   Feedback Connections for Linear m-sequences (excluding
mirror image sequences)

| Number of stages	Code length	Feedback Connections
2	3	[2,1]
3	7	[3,1]
4	15	[4,1]
5	31	[5,2] [5,4,3,2] [5,4,2,1]
6	63	[6,1] [6,5,2,1] [6,5,3,2]
7	127	[7,1] [7,3] [7,3,2,1] [7,4,3,2] [7,6,4,2] [7,6,3,1] [7,6,5,2] [7,6,5,4,2,1] [7,5,4,3,2,1]
8	255	[8,4,3,2] [8,6,5,3] [8,6,5,2] [8,5,3,1] [8,6,5,1] [8,7,6,1] [8,7,6,5,2,1] [8,6,4,3,2,1]
9	511	[9,4] [9,6,4,3] [9,8,5,4] [9,8,4,1] [9,5,3,2] [9,8,6,5] [9,8,7,2] [9,6,5,4,2,1] [9,7,6,4,3,1] [9,8,7,6,5,3]
10	1023	[10,3] [10,8,3,2] [10,4,3,1] [10,8,5,1] [10,8,5,4] [10,9,4,1] [10,8,4,3] [10,5,3,2] [10,5,2,1] [10,9,4,2]
11	2047	[11,1] [11,8,5,2] [11,7,3,2] [11,5,3,2] [11,10,3,2] [11,6,5,1] [11,5,3,1] [11,9,4,1] [11,8,6,2] [11,9,8,3]
12	4095	[12,6,4,1] [12,9,3,2] [12,11,10,5,2,1] [12,11,6,4,2,1] [12,11,9,7,6,5] [12,11,9,5,3,1] [12,11,9,8,7,4] [12,11,9,7,6,5] [12,9,8,3,2,1] [12,10,9,8,6,2]
13	8191	[13,4,3,1] [13,10,9,7,5,4] [13,11,8,7,4,1] [13,12,8,7,6,5] [13,9,8,7,5,1] [13,12,6,5,4,3] [13,12,11,9,5,3] [13,12,11,5,2,1] [13,12,9,8,4,2] [13,8,7,4,3,2]
14	16383	[14,12,2,1] [14,13,4,2] [14,13,11,9] [14,10,6,1] [14,11,6,1] [14,12,11,1] [14,6,4,2] [14,11,9,6,5,2]

binary phase modulated signal is obtained by using phase angles of
zero (a_i = + 1) and 180° (a_i = - 1) for zero and one, respectively.
The fundamental properties of a binary phase coded linear m-sequence
generated by an n-stage generator are [5, 12, 15, 25]:

    (i)   the sequence is periodic with period $N = 2^n - 1$,

    (ii)   in each period, the difference between the number of
ones and the number of minus-ones is one.

    (iii)   half the runs (consecutive states of same kind) are of
length one, one-fourth of length two, etc.,

    (iv)   as a consequence of linearity, if an m-sequence is added
modulo - 2 to a shifted version of itself, the resulting
sum sequence is a shifted version of the original sequence,

    (v)   the periodic correlation is two-valued; i.e.,

$$\sum_{k=1}^{N} a_k a_{i+k} = N \quad \text{if } i = 0, \pm N, \pm 2N, \text{ etc.} \qquad (7.6)$$
$$= - 1, \text{ otherwise.}$$

Non-periodic m-sequences are obtained by retaining just one period
of the periodic version. Different sequences can be obtained by trun-
cating the output after N samples and using different initial conditions.
For an n-stage register, $(2^n - 1)$ different initial conditions are pos-
sible since the all-zero state is not allowed. Figures 7.3(b) - 7.3(h)
show the effect of the initial condition on the autocorrelation function of
the m-sequence produced by the 3-stage generator shown in Figure 7.3(a)
[14, 49]. As can be easily seen, the peak side lobe and its proximity
to the main peak vary widely with the initial condition. Similarly,
sequences generated using different feedback connections also have
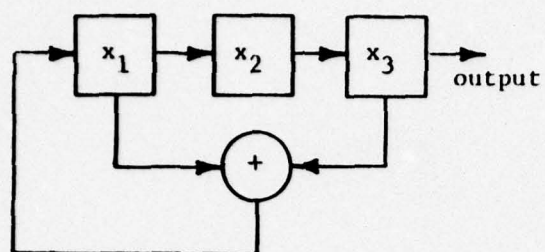
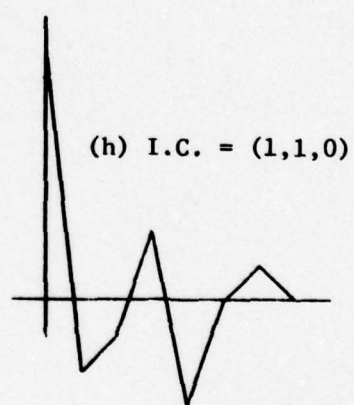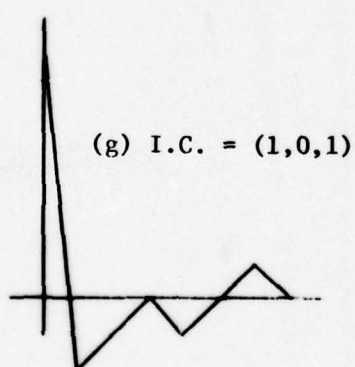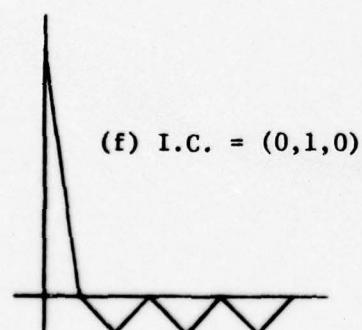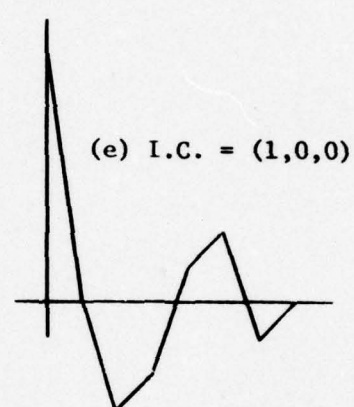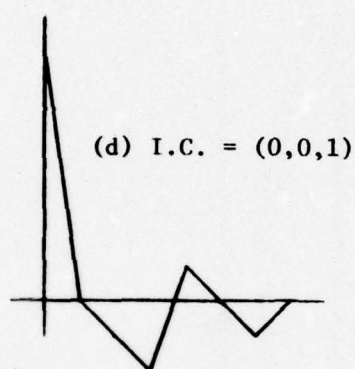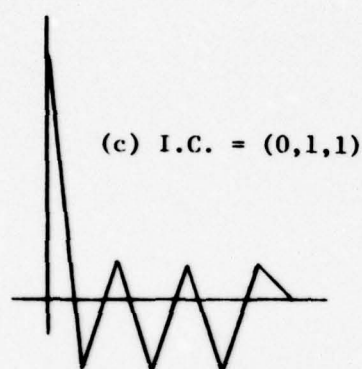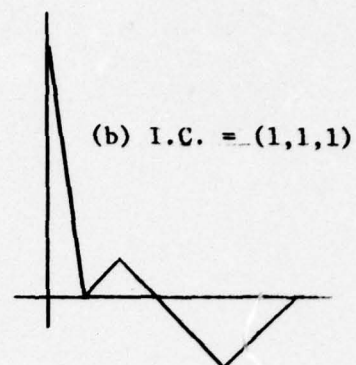Figure 7.3 Effect of Initial Conditions on the autocorrelation of m-sequences

different autocorrelation functions. There is no theoretical tool available to aid in the selection of the feedback connection and the initial condition that will result in a desirable autocorrelation function. To study the effect of doppler mismatch, the correlation functions were computed for an m-sequence generated by a 5-stage generator with feedback connection [5,3] and initial condition (1, 0, 1, 0, 1). Figure 7.4 shows a cutaway section of the uncertainty function for doppler limits of

$$-\frac{2\pi}{10\delta} < \omega_d < \frac{2\pi}{10\delta} .$$

For purposes of comparison, a few slices of this function are shown in Figures 7.5(a) - 7.5(g). Only positive values of τ and ω_d are shown in these figures since the uncertainty function is a symmetric function of both τ and ω_d. For large values of N, the peak-to-side lobe ratio at zero doppler approaches $\sqrt{N}$ (compare with N for Barker codes and $\pi\sqrt{N}$ for Frank polyphase codes). As mentioned earlier, the range side lobe structure is different for different initial conditions. Table 7.2 shows the initial conditions for some of the linear m-sequence generators which yield the largest peak-to-side lobe ratio [43, 54].

The range side lobes may be further reduced by the use of a weighting filter similar to the one employed in the case of Barker codes. The performance of m-sequences in the presence of doppler mismatch is clearly superior to that of the Barker code since it has no appreciable spurious peaks.

For an n-stage SRG, 2^n linear feedback combinations are possible. Only a few of these produce maximal length sequences, others resulting
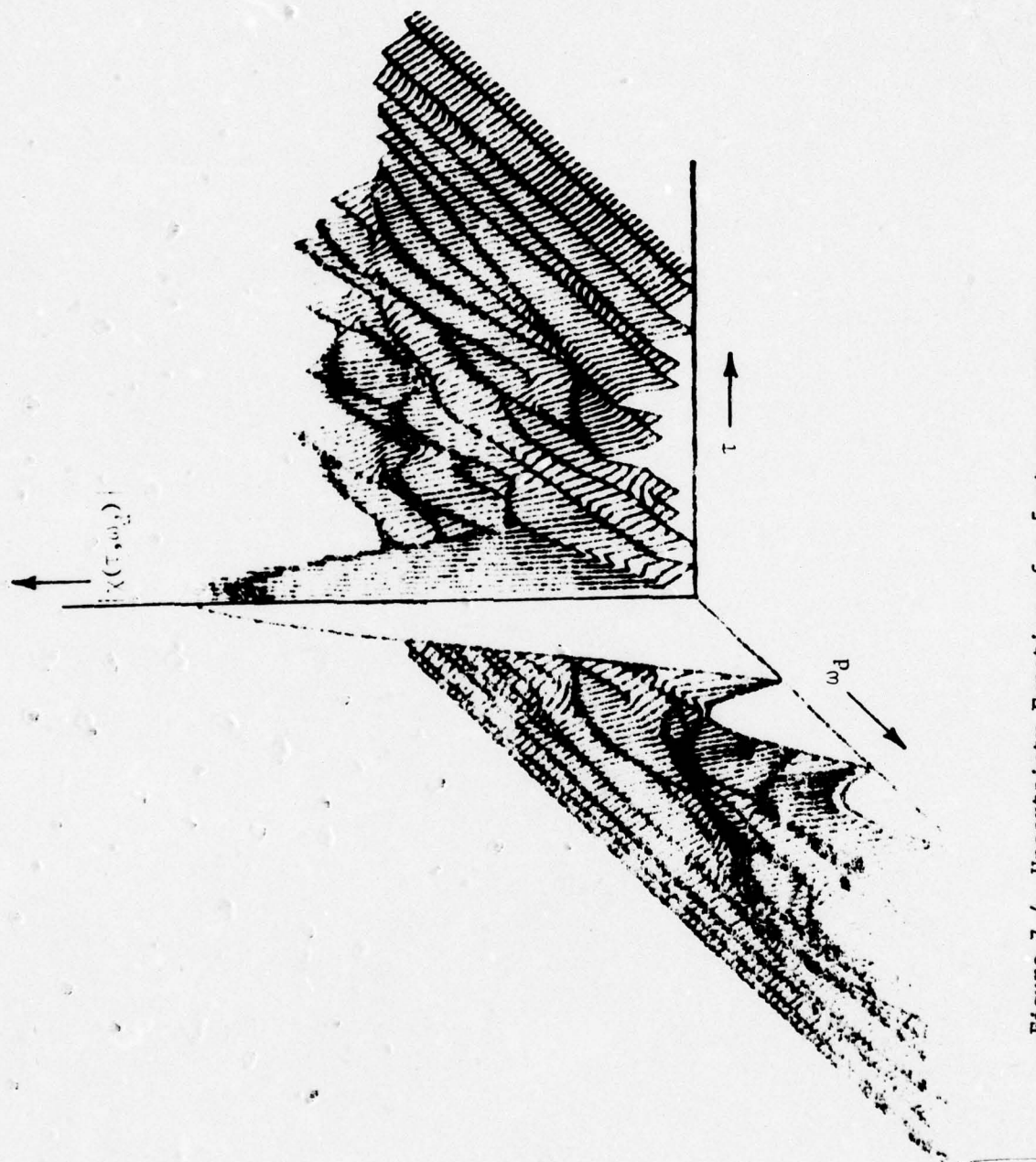
Figure 7.4 Uncertainty Function of a 5-stage m-sequence

(a) $\frac{\omega_d \delta}{2\pi} = 0.0$

(b) $\frac{\omega_d \delta}{2\pi} = 0.005$

(c) $\frac{\omega_d \delta}{2\pi} = 0.01$
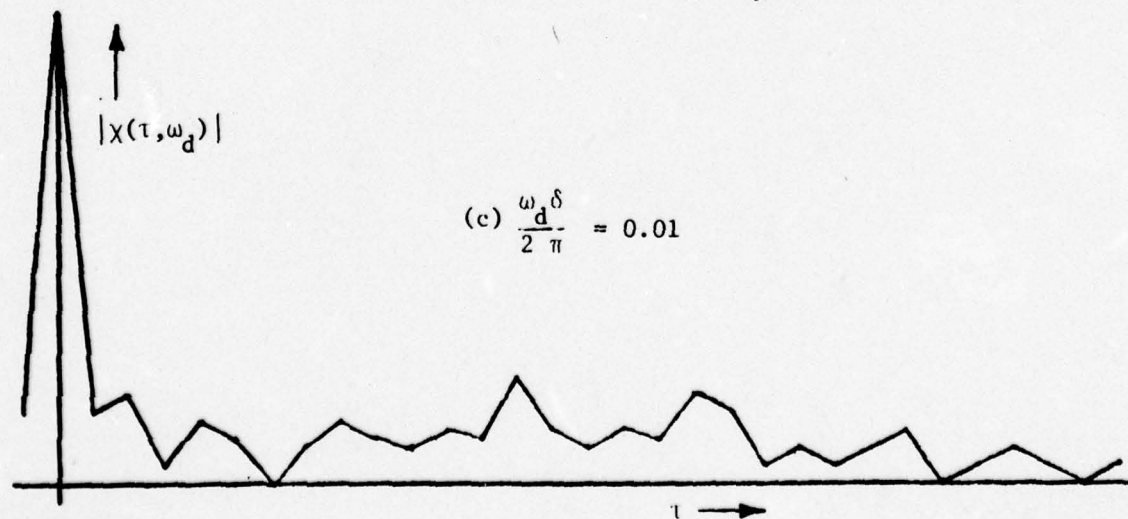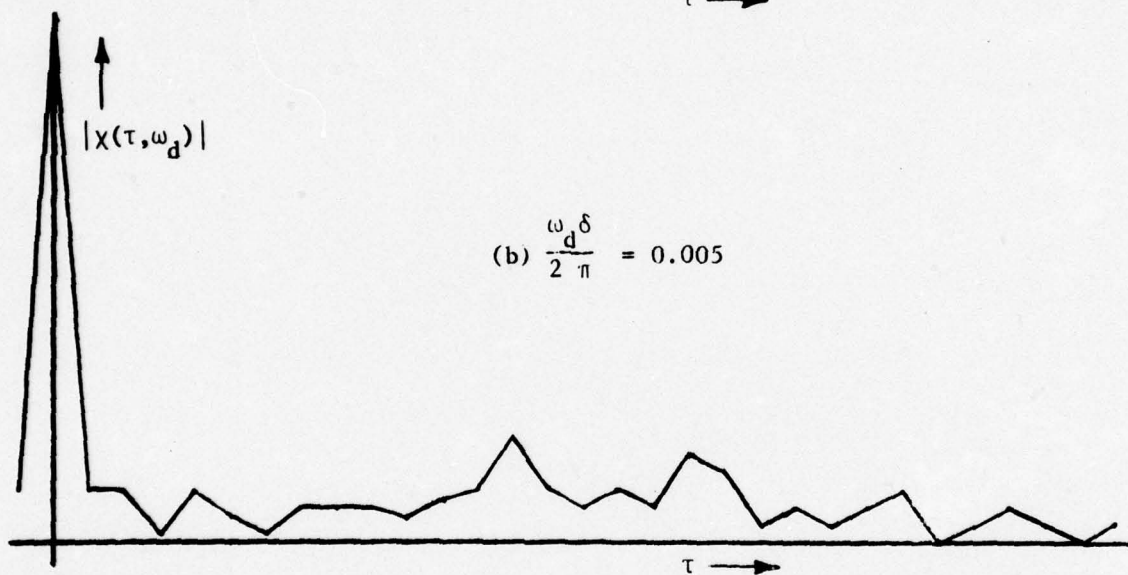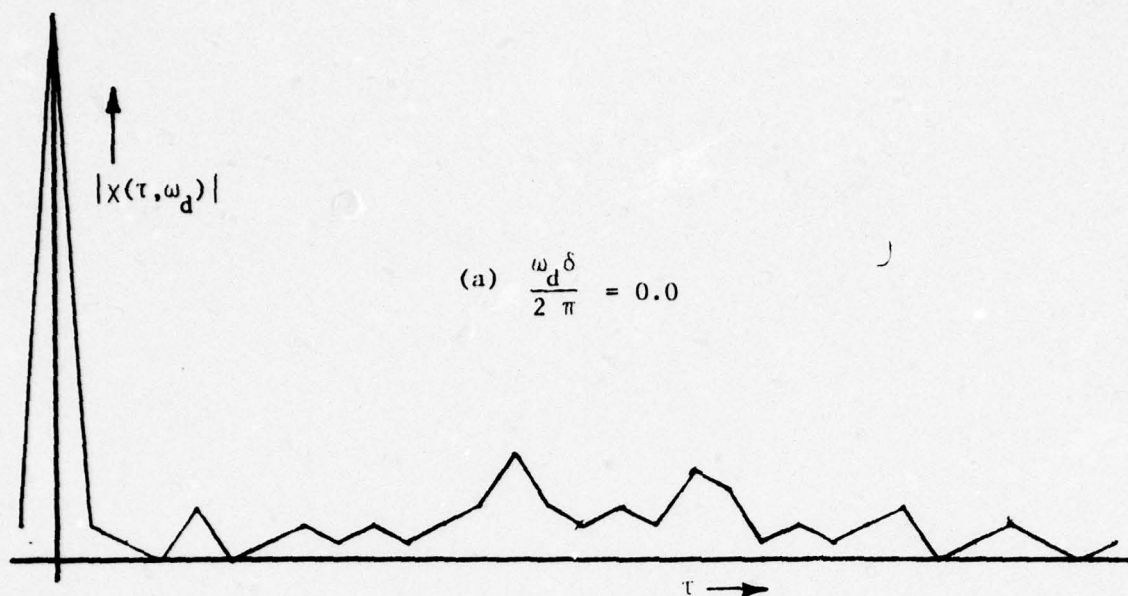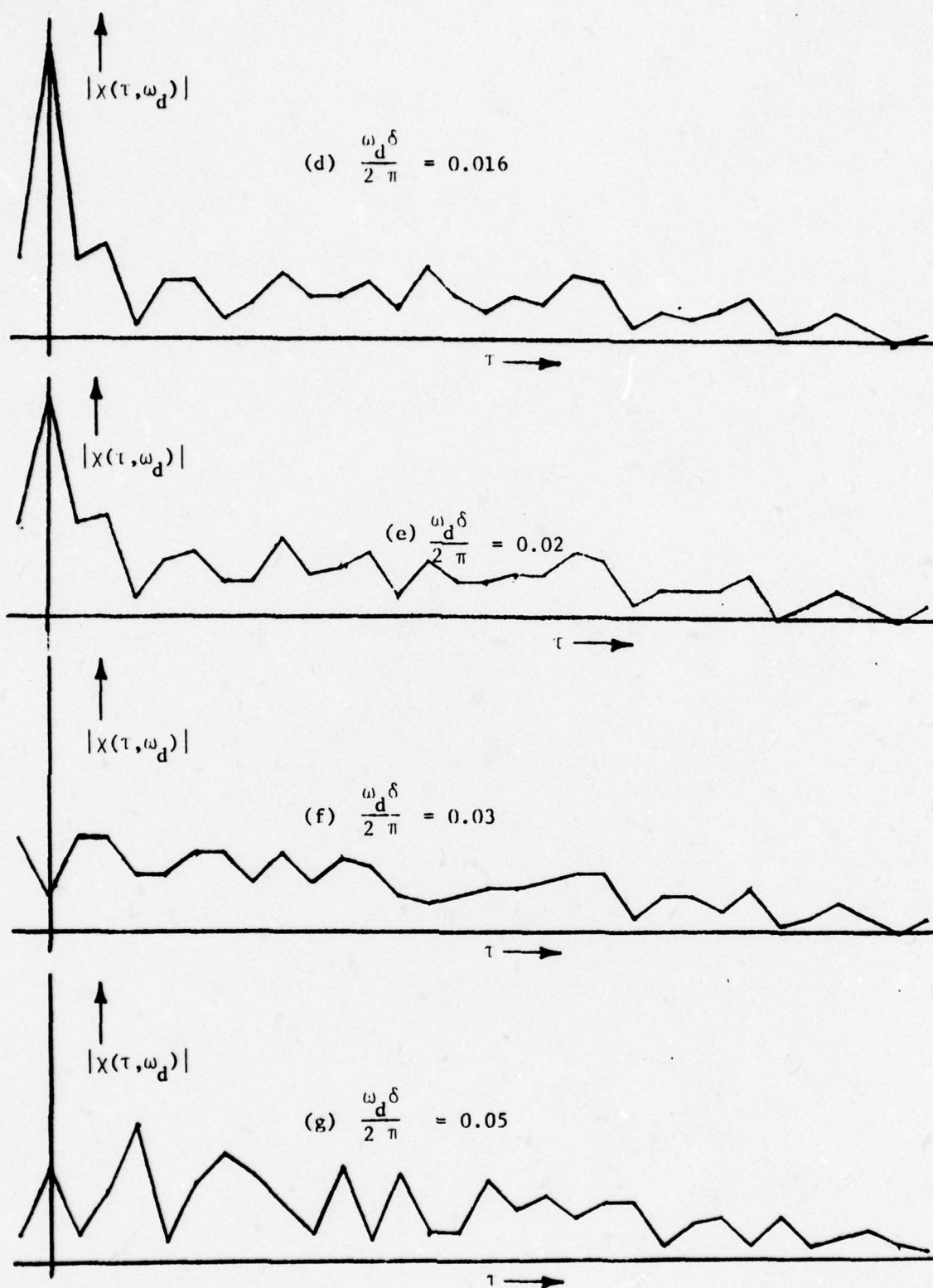
Figure 7.5 Slices of the Uncertainty Function of a 5-stage m-sequence

TABLE 7.2 OPTIMUM INITIAL CONDITIONS

Number of Stages, n	Code Length, N	Feedback Connection	Initial Conditions	Highest Side Lobe
3	7	[3,1]	(0,1,0)	2
4	15	[4,1]	(1,1,1,1)	
			(1,0,0,0)	
			(0,1,0,0)	
			(1,1,1,0)	3
			(0,1,1,0)	
			(0,0,1,0)	
			(1,0,0,1)	
5	31	[5,2]	(1,1,1,0,1)	
			(1,0,0,1,0)	
			(0,0,1,0,0)	4
			(0,0,0,1,1)	
5	31	[5,4,2,1]	(1,1,1,1,0)	
			(1,0,1,1,0)	4
			(0,0,0,1,0)	
			(1,0,0,1,0)	
5	31	[5,4,3,2]	(0,0,0,1,1)	
			(0,0,1,0,0)	
			(0,1,0,0,1)	
			(1,0,0,1,1)	
			(1,0,0,0,1)	4
			(0,1,0,1,0)	
			(1,0,1,0,1)	
			(0,1,0,1,1)	
			(1,0,1,0,0)	
6	63	[6,1]	(1,1,1,1,1,1)	
			(0,1,1,1,1,1)	
			(1,0,1,1,1,1)	
			(0,1,1,0,0,0)	
			(1,0,0,1,0,0)	6
			(1,1,1,1,1,0)	
			(0,0,1,0,0,1)	
			(0,1,0,0,1,0)	
7	127	[7,3,2,1]	(0,0,1,1,1,0,1)	8
8	255	[8,4,3,2]	(0,1,1,1,0,0,0,1)	13
8	255	[8,6,4,3,2,1]	(0,0,1,1,0,0,0,0)	13

in non-maximal length sequences whose period $p < 2^n - 1$. For a given feedback connection, unlike in the case of the m-sequences, different initial conditions produce sequences of different periods. For a given non-maximal generator, there is a longest period available and it is obtained by loading the register with all zeros except for either the first or last stage [5]. Because of this initial loading, such a sequence is called the impulse response sequence. Very little work has been done on the use of non-maximal length sequence in pulse-doppler radars.

The generation of nonlinear sequences can be considered as falling into two cases: (i) the case where the feedback logic is nonlinear, and (ii) the case where the output of a basic linear generator is altered by nonlinear means. The advantage of nonlinear feedback is that many more sequences of maximum period are possible for a given number of stages. The major disadvantage, however, is the lack of a suitable theory for theoretical analysis of nonlinear generators. It has been shown that there are $_2(2^{n-1} - n)$ nonlinear sequences of maximum period for an n-stage register. In the second method of generating nonlinear sequence, linear m-sequences are combined to form composite codes. Even though these codes are not maximal length sequences, they have other interesting properties which warrant their investigation. The Gold codes [17] are generated by modulo - 2 addition of a pair of linear m-sequences of the same period. The new sequence has the same period as the original sequences but is non-maximal. The Gold codes are usful for generating a large number of codes of a given length. Syncopated-register generators [17] use a technique that

multiplexes two sequences to produce a sequence of much higher period. Two m-sequences are added modulo – 2, except that one of the generators has its clock shifted by half a period with respect to the other clock. If the two generators have r and s stages (r ≠ s), then the period of the composite code is $(2^r - 1)(2^s - 1)$. The JPL ranging codes [17] are similar to the Gold codes but are constructed by modulo – 2 addition of two or more m-sequences whose lengths are relatively prime to one another. The period of the composite sequence is the product of the periods of the original sequences.

One other known class of binary sequence whose periodic correlation is maximum at zero delay and minus-one elsewhere is the Legendre sequence or the Perron sequence [24, 25]. Perron sequences are of period N = 4m–1 when this number is a prime. The binary phase coded signal of this type is defined as

$$a_i = \left(\frac{i}{N}\right) \tag{7.7}$$

where the Legendre symbol $\left(\frac{i}{N}\right)$ is defined as

$$\left(\frac{i}{N}\right) = \begin{cases} 1, \text{ if there is an integer x for which } x^2 = i(\text{mod } N) \\ -1, \text{ otherwise .} \end{cases} \tag{7.8}$$

For example, if m = 3 and N = 11, it can be easily shown that

$$a_i = \begin{cases} +1, \text{ if i is among } 0,1,3,4,5,9 \\ -1, \text{ otherwise} \end{cases} \tag{7.9}$$

and the sequence of length 11 is

+ + – + + + – – – + – .

Except for m = 1 or 2, Perron sequences are not m-sequences. The Perron sequence, like any other periodic sequence, can be generated

by some shift register generator, possibly with a nonlinear feedback logic. Other binary pulse compression codes have been proposed, based on dividing N into residue classes [3, 8]. These codes have been generated for code lengths which are prime numbers, and Table 7.3 shows the lowest achievable peak side lobe levels using these codes. It has been claimed that, for a given code length, such a code produces the lowest possible side lobe level.

TABLE 7.3 SIDE LOBE LEVELS FOR RESIDUE CLASS SEQUENCES [8]

Code Length	Lowest Achievable Side Lobe	Code Length	Lowest Achievable Side Lobe	Code Length	Lowest Achievable Side Lobe
7	1	41	4	79	6
11	1	43	4	83	6
13	1	47	4	89	6
17	2	53	5	97	7
19	2	59	5	101	6
23	3	61	5	103	8
29	4	67	5	107	7
31	3	71	5	109	8
37	4	73	6	113	7

8. Complementary Sequences

A set of complementary sequences [11, 23, 60] is defined as a pair of equally long, finite sequences of two kinds of elements which have the property that the number of pairs of like elements with any given separation in one series is equal to the number of pairs of unlike elements with the same separation in the other series. When the two elements of the series are taken to be +1 and -1, it follows immediately that the sum of their two respective autocorrelations is zero except at zero lag. For example, the two sequences

$$A = - + + - + - + + + -$$ (8.1)

and $$B = - + + + + + + - - -$$ (8.2)

are complementary since A has 3 pairs of like adjacent elements and B has 3 pairs of unlike adjacent elements, A has 4 pairs of like alternate elements and B has 4 pairs of unlike alternate elements, and so on. The autocorrelations of A and B can be easily seen to be

$$\rho_A = (1, -2, -1, 2, 1, 0, -1, 0, -3, 10, -3, 0, -1, 0, 1, 2, -1, -2, 1)$$ (8.3)

$$\rho_B = (-1, 2, 1, -2, -1, 0, 1, 0, 3, 10, 3, 0, 1, 0, -1, -2, 1, 2, -1)$$ (8.4)

and
$$\rho_A + \rho_B = (0, 0, 0, 0, 0, 0, 0, 0, 0, 20, 0, 0, 0, 0, 0, 0, 0, 0, 0).$$ (8.5)

The necessary conditions for the existence of complementary sequences are [23]: (i) that the code length N be even, and (ii) that N must be expressible as a sum of, at most, two squares. Existence of complementary

sequences has been established when N is a power of two. Otherwise, they have been discovered only for N of the type

$$N = 10 \cdot 2^n, \qquad \text{for } n \geq 0 .$$

The following are the general properties of complementary sequences:

(i)   The numbers of elements in the two sequences are equal.

(ii)   The two complementary sequences are interchangeable.

(iii)   The order of elements of either or both the sequences may be reversed without affecting the complementary property.

(iv)   Each element of one or both the sequences may be multiplied by -1.

(v)   Alternate elements of both the sequences may be multiplied by -1 without affecting the complementary property.

Thus a single pair of complementary sequences can be the basis for the construction of several pairs of complementary series using the above properties.

Beginning with a few pairs of complementary sequences, it is possible to construct a variety of longer series by simple combinations [23, 42, 62]. Let $A = (a_1, a_2, \cdots, a_N)$ and $B = (b_1, b_2, \cdots, b_N)$ be complementary with all their elements either $+1$ or -1. Also, let $b_i' = -b_i$ and B' denote the series obtained by multiplying every element by -1. In addition, if c_k is -1, then A^{c_k} is taken to be A' and $A^{c_k} = A$ if $c_k = +1$. Longer complementary sequences can then be formed as follows:

(i)   The two series S_1 and S_2 of length $2N$, where

$$S_1 = (A,B) = (a_1, a_2, \cdots, a_N, b_1, b_2, \cdots, b_N)$$

$$(8.6)$$

and

$$S_2 = (A,B') = (a_1, a_2, \cdots, a_N, b_1', b_2', \cdots, b_N')$$

$$(8.7)$$

are complementary.

(ii) The interleaved series T_1 and T_2 of length 2N, where

$$T_1 = (a_1, b_1, a_2, b_2, \cdots, a_N, b_N) \qquad (8.8)$$

and

$$T_2 = (a_1, b_1', a_2, b_2', \cdots, a_N, b_N') \qquad (8.9)$$

are complementary.

(iii) If $C = (c_1, c_2, \cdots, c_M)$ and $D = (d_1, d_2, \cdots, d_M)$ are complementary (note $N = M$ is not required), then the two *two series* U_1 and U_2 of length 2NM where

$$U_1 = (A^{c_1}, A^{c_2}, \cdots, A^{c_M}, B^{d_1}, B^{d_2}, \cdots, B^{d_M})$$

$$(8.10)$$

and

$$U_2 = (A^{d_M}, \cdots, A^{d_2}, A^{d_1}, B^{c_M'}, \cdots, B^{c_2'}, B^{c_1'})$$

$$(8.11)$$

are complementary. Similarly, the two series

$$V_1 = (A^{c_1}, B^{d_1}, A^{c_2}, B^{d_2}, \cdots, A^{c_M}, B^{d_M}) \qquad (8.12)$$

and

$$V_2 = (A^{d_M}, B^{c_M'}, \cdots, A^{d_2}, B^{c_2'}, A^{d_1}, B^{c_1'}) \qquad (8.13)$$

are also complementary.

(iv) Let N be of the type $N = 2^n$. Let the two sequences be partitioned into $L = 2^\ell$ sequences ($\ell \le n$) of equal length such that

$$A = (A_1, A_2, \cdots, A_L) \tag{8.14}$$

and

$$B = (B_1, B_2, \cdots, B_L) . \tag{8.15}$$

Then the two series W_1 and W_2 of length 2N, where

$$W_1 = (A_1, B_1, A_2, B_2, \cdots, A_L, B_L) \tag{8.16}$$

and

$$W_2 = (A_1, B_1', A_2, B_2', \cdots, A_L, B_L') \tag{8.17}$$

are complementary. Note that $\ell = 0$ yields the series S_1

and S_2 whereas $\ell = n$ produces the series T_1 and T_2 .

Thus using the above construction procedure and the general proper-
ties listed earlier, a variety of complementary sequences can be generated.
It must be noted, however, that even though the autocorrelations of two
complementary series add up to zero at non-zero delays, the individual
autocorrelation structures and the cross-correlation between the two
series vary widely between different series of the same length. Four
methods have been suggested for the utilization of complementary sequences
in pulsed radars.

Method 1 [19]: Here the two complementary sequences are transmitted
simultaneously. The two received waveforms are then correlated using
two different matched filters, each matched to one of the sequences.
The outputs of the two filters are then added to yield the final out-
putput. In the absence of noise and doppler mismatch, the outputs of
the two matched filters are the autocorrelations of the two sequences,
and hence the final output will have one peak at a delay corresponding
to the target range and is zero elsewhere.

Method 2 [42]: Instead of simultaneous transmission, the two sequences of a complementary pair may be alternated on successive PRF intervals. The receiver contains two matched filters matched to each of the sequences, and the received signal is passed through the filter corresponding to the code transmitted in that interval. The matched filter outputs for several PRF intervals are then added together (integrated). In the absence of noise and target motion, assuming that an even number of pulses are integrated, the output contains a single peak and is zero elsewhere. However, the cancellation performance is extremely doppler sensitive and doppler correction must be applied. Also, the difference in target range between two intervals results in a relative shift at the matched filter outputs, contributing to poor side lobe cancellation. Thus it is necessary to compensate for the target motion both in range and in doppler. If the integration is performed by an analog device, its frequency response is also important. Rather than alternating the two sequences, equal numbers of the two codes may be used in different sequencing patterns. Different patterns alter the frequency spectrum of the side lobe energy making it more or less suitable for the particular device being used for integration. It is also conceivable that several different pairs of complementary sequences could be used within an integration period.

The two methods described above were proposed for a general radar application. The following two methods are designed specifically for tracking applications where large side lobes are tolerable if they are far away from the main lobe.

Method 3 [11]: Let

$$A = (a_1, a_2, \cdots, a_N) \tag{8.18}$$

and $B = (b_1, b_2, \cdots, b_N)$ (8.19)

be a pair of complementary sequences. Consider the sequence C of length 2N+K such that

$$C = (c_1, c_2, \cdots, c_{2N+K}) \qquad\qquad (8.20)$$

where

$c_i = a_i$ for $i \leq N$

$c_i = 0$ for $N < i \leq N+K$ (8.21)

and $c_i = b_{i-N-K}$ for $N+K < i \leq 2N+K$.

Using the fact that A and B are complementary, the autocorrelation of C can be easily shown to be

$\rho_c(0) = 2N$

$\rho_c(j) = 0$ for $1 \leq j \leq K$ (8.22)

$\rho_c(j) = \rho_{ba}(N-j+K)$ for $K \leq j \leq 2N+K$

where ρ_{ba} denotes the cross-correlation between B and A. For example, let $A = (1, 1, -1, 1)$ and $B = (1, 1, 1, -1)$, $N = 4$ and $K = 5$. Then,

$$C = (1, 1, -1, 1, 0, 0, 0, 0, 0, 1, 1, 1, -1) \qquad (8.23)$$

and $\rho_c = (-1, 0, 3, 0, 1, 0, 1, 0, 0, 0, 0, 0, 8, 0, 0, 0, 0, 0, 1, 0, 1, 0, 3, 0, -1)$.

                       (8.24)

Thus the effect of inserting 5 zeros between A and B is to achieve an autocorrelation with zero side lobes in the interval [-5, 5]. Figure 8.1(a) and 8.1(b) depict the signal and the corresponding autocorrelation function. As can be seen, the autocorrelation is precisely the type desired for tracking applications. The main disadvantage of such
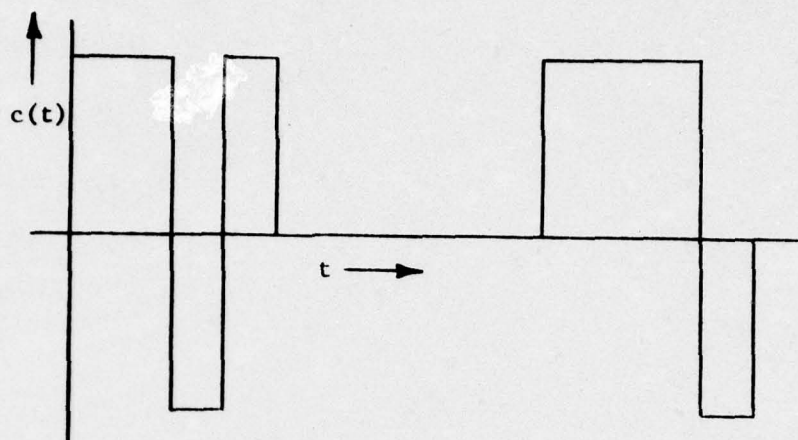
(a) The Original Sequence
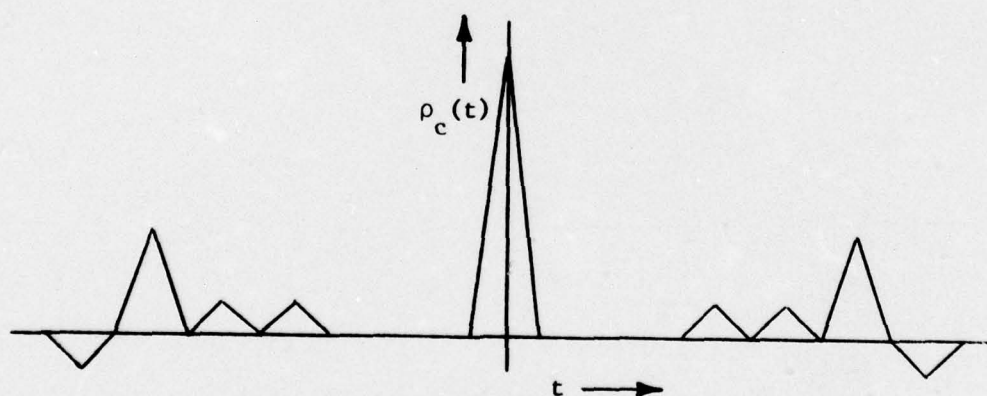
(b) Autocorrelation Function

Figure 8.1 Effect of Inserting Zeros Between two Complementary Series

a waveform is that the signal power utilization efficiency decreases as K increases since no signal is transmitted during the period between the two pulses. However, if the radar is an electronically-steered multipurpose radar, it is possible for the radar to perform some other function during the period between the pulses. In such an application, by selecting K large enough, the signal may also be useful during search operations.

Method 4 [11]: Let A and B be a pair of complementary sequences of length N and consider the code C of length 4MN formed as follows:

$$C = \underbrace{(A, B, A', B, \cdots)}_{\substack{\text{repeated} \\ \text{M times}}} . \tag{8.25}$$

The peak value of the autocorrelation occurs at zero lag and is given by

$$\rho_c(0) = 4MN . \tag{8.26}$$

Since the code is formed by a periodic repetition, $\rho_c(j)$ must have large side lobes when j is a multiple of the period 4N. Using the property that A and B are complementary, the autocorrelation of C in the region $0 < j < 4M$ can be written as follows:

$$\rho_c(j) = - \rho_{ab}(N - j) \quad \text{for } 0 < j \leq N$$

$$\rho_c(j) = - \rho_{ab}(N - j) + (2M - 1) [\rho_b(2N - j) - \rho_a(2N - j)] \quad \text{for } N < j \leq 2N$$

$$\rho_c(j) = + \rho_{ab}(j - 3N) + (2M - 1) [\rho_b(2N - j) - \rho_a(2N - j)] \quad \text{for } 2N < j \leq 3N$$

$$\rho_c(j) = \rho_{ab}(j - 3N) \quad \text{for } 3N < j \leq 4N . \tag{8.27}$$

Therefore, in the region $0 < j \leq N$, the autocorrelation of C is governed by the cross-correlation between the sequences A and B. For the tracking application, let the region of interest be $-K \leq j \leq K$ where $K \leq N$, and let

$$q_{ba} = \max_{j \leq k} |\rho_{ab}(N - j)| \; ; \tag{8.28}$$

then the peak-to-side lobe ratio in the region $[-K, K]$ is

$$\frac{\rho_c(0)}{q_{ba}} = \frac{4MN}{q_{ba}} \; . \tag{8.29}$$

This quantity has a lower bound of 4M and can be maximized by minimizing q_{ba}. Therefore, the best pair of complementary sequences is one where the cross-correlation is small in the region of interest. One must note here that the region of low side lobes cannot be extended beyond $j = N$ because of the autocorrelation structure. Other series combinations of complementary sequences could be considered but no useful results have been published.

9. Simultaneous Amplitude and Phase Modulation
[13, 28, 33, 56]

In all of the codes considered in the previous sections, the pulse amplitude was held constant while its phase was varied. The Huffman codes [11, 33] are made up of finite sequences of amplitude and phase modulated pulses. The complex representation of such a signal can be written for an arbitrary N as

$$\psi(t) = u(t) \, e^{j\omega_0 t} \tag{9.1}$$

$$\text{where } u(t) = \sum_{n=1}^{N} a_n R_n(t) \tag{9.2}$$

$$R_n(t) = 1 \quad \text{for } (n - \delta) \leq t \leq n\delta$$

$$= 0 \quad \text{elsewhere} \tag{9.3}$$

$$\text{and} \quad T = N\delta . \tag{9.4}$$

The excitation sequence $(a_1, a_2, \cdots, a_N)$ consists of complex numbers whose magnitudes and phases are not necessarily equal. The magnitude variation provides the amplitude modulation and the phase variation results in the phase modulation. The elements of the complex excitation sequence are chosen in such a way that the autocorrelation has a desirable structure. In the case of Huffman codes, the autocorrelation of the sequence $A = (a_1, a_2, \cdots, a_N)$ is restricted to be

$$\rho_a(0) = E = \sum_{k=1}^{N} |a_k|^2$$

$$\rho_a(j) = 0 \text{ for } 0 < |j| < N - 1 \tag{9.5}$$

$$\rho_a(N - 1) = a_1^* a_N = \pm 1$$

and $\rho_a(-(N-1)) = a_1 a_N^* = \pm 1$

where E is the energy. Because of this autocorrelation structure, these sequences are also called impulse equivalent sequences. If $A(z)$ is the Z-transform of $\{a_n\}$ and $P(z)$ is the Z-transform of the autocorrelation $\rho_a(j)$, then it can be easily shown that

$$P(z) = A(z) \, A^*(z^{-1}) \tag{9.6}$$

where

$$A(z) = a_1 + a_2 z^{-1} + a_3 z^{-2} + \cdots + a_N z^{-(N-1)} \tag{9.7}$$

and

$$P(z) = \sum_{j=-(N-1)}^{N-1} \rho_a(j) z^{-j} \ . \tag{9.8}$$

Substituting for $\rho_a(j)$ from (9.5), $P(z)$ becomes

$$P(z) = a_1 a_N^* \, z^{N-1} + E + a_1^* a_N z^{-(N-1)} \ . \tag{9.9}$$

The 2N-2 roots of (9.9) can be shown to be as follows:

(i) If $a_1^* a_N = -1$,

$$z_k^{-1} = R_1 e^{jk\phi} \qquad \text{for } 0 \le k \le N-2 \tag{9.10}$$

$$z_k^{-1} = R_2 e^{j(k-N+1)\phi} \qquad \text{for } N-1 \le k \le 2N-2 \tag{9.11}$$

(ii) If $a_1^* a_N = +1$,

$$z_k^{-1} = R_1 e^{j(k+0.5)\phi} \qquad \text{for } 0 \le k \le N-2 \tag{9.12}$$

$$z_k^{-1} = R_2 e^{j(k-N+1+0.5)\phi} \qquad \text{for } N-1 \le k \le 2N-2 \tag{9.13}$$

where

$$\phi = \frac{2\pi}{N-1} \tag{9.14}$$

$$R_1^{N-1} = \frac{E}{2} + \sqrt{\frac{E}{2}^2 - 1} \tag{9.15}$$

$$R_2 = \frac{1}{R_1} \quad \cdot \tag{9.16}$$

Therefore, the roots lie on two concentric circles centered at the origin and are equally spaced around the circles. There are N-1 pairs of roots where each pair consists of one root on the inner circle and one on the outer circle along the same radial line. One of each pair of these roots can be assigned to $A(z)$ while the other is automatically assigned to $A*(z^{-1})$. Once the roots of $A(z)$ are known, the corresponding polynomial and hence the excitation sequence can be determined. Since one from each of N-1 pairs are assigned to $A(z)$, there are 2^{N-1} different possible choices of these roots. While every one of these choices results in the same autocorrelation, some yield real sequences and the others result in complex sequences. In addition, each choice results in a different distribution of the amplitudes. For maximum transmission efficiency, the radar should transmit at peak power over the entire duration; i.e., the ideal situation is

$$|a_1| = |a_2| = \cdots = |a_N| = \sqrt{\frac{E}{N}} \quad \cdot \tag{9.17}$$

The choice of the root pattern must be such that the amplitude distribution is as close as possible to the ideal distribution (9.17) . That is, the root pattern must be chosen to maximize the energy utilization ratio [1, 2, 50],

$$\sigma = \frac{E/N}{\max_k |a_k|^2} \quad \cdot \tag{9.18}$$

A computer evaluation has been carried out to determine the optimum root pattern [36]. It has been shown, for example, that for N = 11, the highest possible value of σ is 0.54.

In order to improve the energy utilization ratio, the restriction on the autocorrelation structure can be relaxed. For example, if an additional side lobe pair of amplitude one is allowed to exist one time side lobe width away from the unavoidable end time side lobe pair [35], i.e.,

$$\rho_a(j) = E \text{ for } j = 0$$

$$|\rho_a(j)| = 1 \text{ for } |j| = N - 1$$

$$|\rho_a(j)| = 1 \text{ for } |j| = N - 3 \tag{9.19}$$

$$\rho_a(j) = 0, \text{ otherwise}$$

then, for N = 11, the energy utilization ratio can be increased to 0.624. Thus, in tracking applications, by allowing even more side lobes to exist outside the region of interest, higher energy utilization ratios could be achieved.

Another approximation to the Huffman code is the modified Barker code [34] where the autocorrelation is specified as

$$\rho_a(j) = E \text{ for } j = 0$$

$$|\rho_a(j)| = 1 \text{ for } |j| = N - 1$$

$$|\rho_a(j)| = p \text{ for } |j| = 2,4,6, \cdots \tag{9.20}$$

$$\rho_a(j) = 0, \text{ otherwise } .$$

Clearly, p = 0 yields the Huffman code and p = 1 gives the Barker code if it exists for the given length. The code can be generated for

different values of p using a similar procedure as the Huffman code. The energy utilization ratio increases as p increases from 0 to 1. For example, if $N = 13$, $p = 0$ gives a value of $\sigma = 0.564$ whereas $p = 0.5$ yields $\sigma = 0.713$.

Ternary sequences are amplitude and phase modulated codes where both the amplitude and phase take on one of two values. Specifically, a ternary sequence $\{a_n\}$ consists of elements 1, -1, and zero. Ternary sequences whose cyclic autocorrelation is zero everywhere except at zero lag have been considered. Tompkins [56] managed by brute force technique to generate codes up to length 18. A systematic method for generating ternary sequences is described by Chang [13] when the length of the sequence is given by $N = (3^n - 1)$ where n is odd. The non-periodic autocorrelation of these functions and the effect of doppler mismatch have not been investigated.

10. Binary Coding of In-Phase and Quadrature Components

The complex envelope defined in (3.3) may be written as

$$u(t) = a(t)\, e^{-j\phi(t)}$$

$$= x_d(t) - jx_q(t) \tag{10.1}$$

where $x_d(t)$ and $x_q(t)$ are the in-phase and quadrature components, respectively. The corresponding transmitted signal is

$$s(t;\omega_0) = x_d(t)\cos\omega_0 t + x_q(t)\sin\omega_0 t \quad . \tag{10.2}$$

If both $x_d(t)$ and $x_q(t)$ are binary coded, i.e., if they take on values +1 and -1, then it can be easily seen that

$$a(t) = \sqrt{2} \tag{10.3}$$

and $\quad \phi(t) = \pm\frac{\pi}{4},\quad \pm 3\frac{\pi}{4}\ , \tag{10.4}$

which represents a four-phase code of constant amplitude. Conversely, any four-phase code where the phases are equally separated can be implemented by transmitting a pair of binary coded signals in quadrature. Since good four-phase codes of length greater than 16 are not known, various combinations of binary codes must be tried for $x_d(t)$ and $x_q(t)$.

The autocorrelation of u(t) can be expressed in terms of the auto- and cross-correlation integrals of the in-phase and quadrature components; i.e.,

$$\rho_{uu}(\tau) = (\rho_{dd}(\tau) + \rho_{qq}(\tau)) - j(\rho_{dq}(\tau) - \rho_{qd}(\tau)) \quad .$$

The radar performance depends upon the peak-to-side lobe ratio of $|\rho_{uu}(\tau)|$,

$$|\rho_{uu}(\tau)|^2 = (\rho_{dd}(\tau) + \rho_{qq}(\tau))^2 + (\rho_{dq}(\tau) - \rho_{qd}(\tau))^2 \quad .$$

The problem is to select the binary sequences x_d and x_q which minimize $|\rho_{uu}(\tau)|^2$ for $\delta \leq \tau \leq k\delta$ where k represents the window of interest. At the present time there is no rational method for determining x_d and x_q. Many pairs of (x_d, x_q) were considered. Good results were obtained for symmetric pairs, in which case $\rho_{dq}(\tau) - \rho_{qd}(\tau) = 0$. For example,

$$x_d = + + + + - - + + - + - + - + + - + + - + - + - + + - - + + + +$$

$$x_q = + + - - - - - - - + + - - + - + - + - - + + - - - - - - - + +$$

$$|\rho_{uu}| = (62, 0, 2, 0, 2, 0, 2, 0, 6, \cdots) .$$

More work is required before this technique can be evaluated.

11.   Example of Binary Code Selection

As explained earlier, the criterion for the selection of a code depends upon the application. The PSLR or the peak – to – rms side lobe ratio is appropriate for a search radar. On the other hand, for a radar which is dedicated to acquisition and tracking, only the side lobes in the vicinity of the main lobe are of concern. For example, the selection of the signal may be based upon its autocorrelation at lags 0, δ, 2δ, 3δ, 4δ, and 5δ which corresponds to a total of 10 range cells (one range cell is equivalent to the width of the compressed pulse, δ). The following is a comparison of several binary codes of length 31, where PPO stands for peak-to-side lobe ratio in dB for the entire correlation, PRO is the over-all peak-to-rms side lobe ratio in dB, PPL and PRL are the corresponding quantities within 5 range cells of the main peak.

(i)   Contiguous Barker Codes : A code of length 31 may be formed by arranging Barker codes of length 13, 13, and 5 contiguously. The performance figures for such a code are PPO = 5.7, PRO = 18.2 PPL = 20.3, and PRL = 21.5. Contiguous arrangement of Barker codes of lengths 13, 11, and 7 also yields a code of length 31. For this sequence, PPO = 9, PRO = 18.1, PPL = 20.3, PRL = 26.8.

(ii)   Linear m – sequences : There are 3 feedback connections and 31 possible initial conditions for each connection, yielding a total of 93 linear m – sequences. Only those whose performance is optimum in some sense are mentioned here. There are 17 sequences with the highest PPO of 17.8, the feedback connections and initial conditions of which are given in table 7.2. The sequence with feedback [5,4,3,2] and initial condition (0,1,0,0,1) has the highest PRO which is PRO = 25. The sequence with the

highest PPL and PRL is obtained by the feedback connection [5,2] and initial condition (0,1,1,0,0), and the values are PPL = 29.8 and PRL = 33.8.

(iii)   Residue Class Sequences : Of the many residue class sequences available for N = 31, only a few were analyzed. The important result is that a sequence generated by dividing 31 into 10 residue classes gives a PPO of 20.3 which is larger than that of the best m – sequence and, in fact, is the highest that can be obtained for a binary code of length 31. None of the other sequences studied had larger values for PPL than the best m – sequence given above.

(iv)   Perron Sequences : The residue class sequence obtained using two residue classes is identical to the Perron sequence. No such sequence was found which had better performance than the m – sequences.

(v)   Larger Length Sequences : A sequence of length 35 can be obtained by combining Barker codes of lengths 7 and 5. Such a sequence has PPL = 16.9 and PRL = 19.8. A residue class sequence of length N = 47 was also studied. This sequence has the highest PPL and PRL of all the sequences considered and the values are PPL = 33.4 and PRL = 37.4.

Table 11.1 shows those sequences which are optimum in some sense. The performance of these sequences may be improved further by the use of a weighting filter. Such a filter is especially simple to synthesize for the combined Barker code. The behavior of the binary sequences in the presence of doppler mismatch was not investigated in detail.

TABLE 11.1 OPTIMUM BINARY SEQUENCES

Sequence	Origin	Optimality
--++++++++--+-+++--+-+-++--+-+	Residue Class N = 31	PPO = 20.3
+++++--++++-+-+-+++--+---+	m – sequence N = 31	PRO = 25
++-+-++--+-+---+-+---+++----	m – sequence N = 31	PPL = 29.8 PRL = 33.8
---+-++---++---+++++-+-+++--+--+-+-++	Residue Class N = 47	PPL = 33.4 PRL = 37.4

12. Summary and Conclusions

The following types of pulse compression signals were discussed in this report: (i) linear and nonlinear FM, (ii) polyphase codes, (iii) Barker codes, (iv) shift register generated binary sequences, (v) complementary series, and (vi) codes with simultaneous amplitude and phase modulation. The performance of a pulsed radar is determined by examination of the ambiguity function when a single pulse is involved. The performance may be improved either by integration or by weighting or by both. In the evaluation of a pulse compression signal, the following factors will be considered: (i) signal generation, (ii) peak-to-side lobe ratio (PSLR) of the autocorrelation and the relative location of the first large side lobe, (iii) effect of doppler mismatch, and (iv) applicability of integration and/or weighting.

Linear FM signals can be generated for BT products up to 4000. The PSLR is about 13.5 dB which implies that weighting is required. The first side lobe is the largest. A doppler mismatch causes both a reduction in the PSLR and an error in range measurement. Using weighting techniques, the PSLR can be increased at the expense of a small widening of the main lobe. For example, Hamming weighting can increase the PSLR to 42.8 dB with a main lobe widening factor of 1.47. The PSLR can be increased by using nonlinear FM but the performance becomes very sensitive to doppler mismatch.

Frank polyphase codes are the most important polyphase codes and exist for lengths $N = p^2$. For large values of p, the PSLR approaches πp. For example, $p = 6(N = 36)$ corresponds to PSLR = 25 dB. The polyphase codes have doppler degradations somewhat similar to those of

linear FM. Another interesting type of polyphase code is the generalized Barker sequence where the PSLR = N, the length of the code. Unfortunately, the existence has not been established for lengths larger than 15.

The most useful binary codes are Barker sequences, shift register generated sequences, and complementary series. Barker codes exist only for N = 2,3,4,5,7,11, and 13 and have the unique property that the PSLR is equal to N. The performance deteriorates rapidly for large values of doppler mismatch. Weighting filters can be designed to increase substantially the PSLR. Particularly important to tracking applications is the fact that the first K side lobes can be entirely suppressed by a transversal filter of order 2K. Longer codes can be achieved using multistage Barker codes.

Linear m-sequences are commonly used because they are easily generated by linear shift register generators. An n-stage shift register with proper feedback can generate an m-sequence of length $N = 2^n - 1$. Since the signal is aperiodic, the ambiguity function depends upon the feedback configuration and on the initial condition for a given feedback structure. Initial conditions which produce the largest PSLR have been tabulated. For example, the best m-sequence of length 31 has a PSLR of 12.9 dB. For large values of N, the PSLR approaches $\sqrt{N}$, which can be further increased by the use of a weighting filter similar to the one employed in the case of a Barker code. The performance of m-sequences in the presence of doppler mismatch is superior to that of the Barker code since it has no appreciable spurious peaks.

Another type of binary sequence is the Perron sequence whose periodic correlation is maximum at zero delay and is minus-one elsewhere. Such

sequences exist for lengths of the type $N = 4m - 1$ when this number is prime. Unfortunately, there is no general theory about the aperiodic correlation properties of the Perron sequences.

Residue class sequences have been generated for code lengths which are prime numbers. It has been claimed that such codes produce the largest possible PSLR for a given code length. A definite advantage of these sequences over the m-sequences is that they exist for a larger set of lengths.

It is possible to obtain longer binary sequences by combining two or more binary sequences. It is advantageous to start from a pair of complementary sequences. For example, a code can be formed by repeating M times (A, B, A', B) where A and B are complementary of length N. The PSLR within K (K < N) steps of the main lobe has a lower bound of 4M and can be maximized by minimizing the cross-correlation between A and B. Another proposal was to form a long code by inserting K zeros between two complementary sequences of length N. In this case, the side lobes will be zero within K steps of the main lobe, which is particularly attractive in tracking applications.

Improved performance may be obtained by integration of two or more output pulses. If the matched filter outputs due to two complementary sequences are integrated, the result will have a single peak and will be zero elsewhere (assuming zero doppler mismatch). Two methods were suggested to take advantage of this property. In the first method, the two complementary sequences are transmitted simultaneously. The two received waveforms are then passed through the matched filters, each matched to one of the sequences, and their outputs

are added to yield the final output. In the second method, the two sequences of a complementary pair are alternated on successive PRF intervals and the matched filter outputs for several intervals are integrated. In this case, the performance is extremely doppler sensitive and doppler correction must be applied.

In all the signals considered thus far, higher BT products were accomplished by phase modulation. An alternative scheme to achieve high BT product is simultaneous amplitude and phase modulation. An example of such a signal is the Huffman code which exists for all lengths. If the length of the code is N, then the autocorrelation is maximum at zero lag and is zero elsewhere except at lag $N-1$. Several Huffman sequences are available for a given length, but the best sequence is one which results in the maximum energy utilization ratio, i.e., which has the most uniform amplitude distribution. In tracking applications, other side lobes may be allowed to exist in addition to the ones in the Huffman code. Such sequences can be generated by a procedure similar to the one used for Huffman codes and result in higher energy utilization ratios as compared to the Huffman codes. For example, for $N = 11$, the highest energy utilization ratio for a Huffman code is 0.54, whereas by allowing one more side lobe at lag $N - 3 = 8$, the ratio can be increased to 0.624.

The emphasis of this study has been on binary phase coded signals suitable for tracking applications. As mentioned earlier, a signal can be used in tracking radars even if its autocorrelation has a low PSLR as long as the side lobe levels are small in the vicinity of the main lobe. In view of this criterion, the following conclusions are drawn regarding binary phase coded signals:

(i)   Long codes and hence high compression ratios can be obtained
by combining Barker codes. The advantage of these codes is
that weighting filters can be easily designed to suppress
the side lobes near the main lobe. The critical considera-
tion in evaluating such a code is its sensitivity to doppler
mismatch.

(ii)   Linear m-sequences are easy to generate and are less sensi-
tive to doppler shift than Barker codes. Based either on
theoretical considerations or on exhaustive computer evalua-
tion, optimum m-sequences have been tabulated which yield
the highest PSLR. These codes must therefore be reevaluated
for tracking applications where a high PSLR is not essential.
Furthermore, weighting filters can be designed to improve
their performance.

(iii)   Residue class sequences exist for many more lengths than
the m-sequences. Even though it is claimed that these se-
sequences have the best PSLR for a given length, their
suitability in tracking has not been established.

(iv)   Zero side lobes in the vicinity of the main lobe can be
attained by forming a long code where zeros are inserted
between a pair of complementary sequences. The main draw-
back to such a scheme is the reduced energy utilization
ratio.

(v)   Long codes may be obtained by repeating a pair of comple-
mentary series. In such a situation, the side lobes level
near the main lobe is determined by the cross-correlation

between the two complementary series. The optimum choice of the complementary pair is therefore one that has the smallest cross-correlation. No theoretical tool is available for this optimization, and hence it must be accomplished via a computer search.

(vi) Complementary series may be used in conjunction with pulse integration to yield an improved performance. A pair of complementary series may either be transmitted simultaneously or be alternated on successive PRF intervals, and the outputs integrated. In the absence of doppler shift, all the side lobes are completely suppressed.

(vii) It was shown that a four-phase modulation can be easily obtained by binary modulation of both in-phase and quadrature components. However, no rational method for the selection of the pair of sequences has yet been developed.

(viii) The selection of binary codes of length 31, 35, and 47 was discussed, resulting in the recommendation of optimum codes where both local and overall performances were considered.

Of course, better performance may be obtained by using signals other than binary phase coded signals. Examples of such signals are the poly-phase codes and signals with simultaneous amplitude and phase modulation. Invariably the improvement in performance is attained at the expense of increased complexity and cost of implementation.

LIST OF REFERENCES

1. Ackroyd, M. H.," The Design of Huffman Sequences," IEEE Trans. AES, Vol. AES-6, Nov. 70, pp 790.

2. Ackroyd, M. H.," Synthesis of Efficient Huffman Sequences," IEEE Trans. AES, Vol. AES-8, Jan. 72, pp 2.

3. Archibald, R. G., _An Introduction to the Theory of Numbers_, Merril Publishing Co., New York, 1970.

4. Barton, D. K.(Ed), _Radars (5 Volumes)_, Artech House, Dedham, Mass., 1975.

5. Berkowitz, R. S., _Modern Radar_, John Wiley & Sons, New York, 1967.

6. Birdsall, T. G. and M. P. Ristenbatt, _Introduction to Linear Shift-Register Generated Sequences_, Univ. of Michigan, Ann Arbor, Oct. 58.

7. Blackband, W. T.(Ed), _Radar Techniques for Detection, Tracking and Navigation_, Gordon and Breach, New York, 1966.

8. Boehmer, A. M.," Binary Pulse Compression Codes," IEEE Trans. IT, Vol. IT-13, Apr. 67, pp 156.

9. Braasch, R. H. and A. Erteza," A Recursion for Determining Feedback Formulas for Maximal Length linear pseudo-Random Sequences," Proc. IEEE, Vol. 54, Jul. 66, pp 999.

10. Burdic, W. S., _Radar Signal Analysis_, Prentice-Hall, Englewood Cliffs, N.J., 1968.

11. Caprio, J. R., _On Optimum Radar Ranging Codes_, Ph.D. Thesis, Cornell University, Sep. 66.

12. Chandler, J. P., _An Introduction to Pseudo-Noise Modulation_, Harry Diamond Lab. Rept., Washington D.C., Jan. 64.

13. Chang, J. A.," Ternary Sequences with Zero Correlation," Proc. IEEE, Vol. 55, Jul. 67, pp 1211.

14. Cook, C. E. and M. Bernfeld, _Radar Signals_, Academic Press, New York, 1967.

15. DeLong, D. F., _Experimental Autocorrelation of Binary Codes_, MIT Lincoln Lab. Tech. Rept. No. 47G-0006, Oct. 60.

16. DeLong, D. F., _Three Phase Codes_, MIT Lincoln Lab. Tech. Rept. No. 47.28, Jul. 59.

17. Dixon, R. C., _Spread Spectrum Techniques_, John Wiley & Sons, New York, 1976.

18. Elspas, B., <u>A Radar System Based on Statistical Estimation and Resolution Considerations</u>, Appl. Electron. Lab. Stanford. Univ. Tech. Rept. No. 361-1, Aug. 55.

19. Erickson, C. W., <u>Clutter Cancelling in Autocorrelation Functions by Binary Sequence Pairing</u>, US Navy Electron. Lab., NEL Rept. No. 1047, 1961.

20. Fowle, E. N., <u>The Design of Radar Signals</u>, Mitre Corp. Tech. Rept. No. SR-98, Nov. 63.

21. Frank, R. L.," Polyphase Codes with Good Nonperiodic Correlation Properties," IEEE Trans. IT, Vol. IT-9, Jan. 63, pp 43-

22. Frank, R. L. and S. A. Zadoff," Phase Shift Pulse Codes with Good Periodic Correlation Properties," IRE Trans. IT, Vol. IT-8, Oct. 62, pp 381.

23. Golay, M. J. E.," Complementary Series," IRE Trans. IT, Vol. IT-7, Apr. 61, pp 82.

24. Golomb, S. W., <u>Sequences with Randomness Properties</u>, Martin Co., Baltimore, Maryland, Jun. 55.

25. Golomb, S. W., <u>Shift Register Sequences</u>, Holden Day, Inc., New York, 1967.

26. Golomb, S. W. and R. A. Scholtz," Generalized Barker Sequences," IEEE Trans. IT, Vol. IT-11, Oct. 65, pp 533.

27. Heimiller, R. C.," Phase Shift Pulse Codes with Good Periodic Correlation Properties," IEEE Trans. IT, Vol. IT-7, Oct. 61, pp 254.

28. Hofstetter, E. M.," Construction of Time-Limited Functions with Specified Autocorrelation Functions," IEEE Trans. IT, Vol. IT-10, Apr. 64, pp 119.

29. Hollis, E. E.," Comparison of Combined Barker Codes for Coded Radar Use," IEEE Trans. AES, Vol. AES-3, Jan. 67, pp 141.

30. Hollis, E. E.," Predicting the Truncated Autocorrelation Functions of Combined Barker Sequences of Any Length Without the Use of a Computer," IEEE Trans. AES, Vol. AES-3, Mar. 67, pp 368.

31. Hovanessian, S. A., <u>Radar Detection and Tracking Systems</u>, Artech House, New York, 1973.

32. Howard, T. B.," Application of some Linear FM Results to Frequency Diversity Wavwforms," RCA Review, Mar. 1965.

33. Huffman, D. A.," The Generation of Impulse-Equivalent Pulse Trains," IEEE Trans. IT, Vol. IT-8, Sep. 62, pp S10.

34. Huffman, D. L.," Modified Barker Code Approximating Huffman's Impulse-Equivalent Sequence," IEEE Trans. AES, Vol. AES-11, Jul. 75, pp 437.

35. Huffman, D. L.," A Modification of Huffman's Impulse-Equivalent Pulse Trains to Increase Signal Energy Utilization," IEEE Trans IT, Vol. IT-20, Jul. 74, pp 559.

36. Huffman, D.L.," A Computer Evaluation of Huffman Codes," NAECON 1973, pp 159.

37. Jacobus, R. W., A Linear FM 1000:1 Pulse Compression System, Mitre Corp. Rept. No. ESD-TDR-63-237, Jul. 63.

38. Key, E. L. et at., A Method of Side Lobe Suppression in Phase Coded Pulse Compression Systems, MIT Lincoln Lab. Rept. No. 209, Aug. 59.

39. Luenberger, D. G.," On Barker Codes of Even Length," Proc. IEEE, Vol. 51, Jan. 63, pp 230.

40. Lurin, E. S.," Digital Pulse Compression Using Polyphase Codes," Proc. IEEE, Vol. 51, Sep. 63, pp 1262.

41. Mohanty, N. C.," Multiple Frank-Heimiller Signals for Multiple Access Systems," IEEE Trans. AES, Vol. AES-11, Jul. 75, pp 622.

42. Mutton, J. O.," Advanced Pulse Compression Techniques," NAECON 1975, pp 141.

43. Nathanson, F. E., Radar Design Principles, McGraw-Hill, New York, 1969.

44. Peebles, P. Z. et al.," A Technique for the Generation of Highly Linear FM Pulse Radar Signals," IEEE Trans. MIL, Vol. MIL-9, Jan. 65, pp 32.

45. Persons, C. E.," Ambiguity Function of Pseudo-Random Sequences," Proc. IEEE, Vol. 54, Dec. 66, pp 1946.

46. Rihaczek, A. W. and R. M. Golden," Range Side Lobe Suppression for Barker Codes," IEEE Trans. AES, Vol. AES-7, Nov. 71, pp 1087.

47. Rihaczek, A. W., Principles of High Resolution Radar, McGraw-Hill, New York, 1969.

48. Roth, H. H.," Linear Binary Shift Register Circuits Utilizing a Minimum Number of Mod-2 Adders," IEEE Trans. IT, Vol. IT-11, Apr. 65, pp 215.

49. Sakamoto, T. et al.," Coded Pulse Radar System," J. of the Faculty of Eng., Univ. of Tokyo, Vol. XXVII, 1964, pp 119.

50. Schroeder, M. R.," Synthesis of Low-Peak-Factor Signals and Binary Sequences with Low Autocorrelation," IEEE Trans. IT, Vol. IT-16, Jan. 70, pp 85.

51. Skolnik, M. I., <u>Introduction to Radar Systems</u>, McGraw-Hill, New York, 1962.

52. Skolnik, M. I.(Ed), <u>Radar Handbook</u>, McGraw-Hill, New York, 1970.

53. Storer, J. E. and R. Turyn," Optimum Finite Code Groups," Proc. IRE , Vol, 46, Sep. 58, pp 1649.

54. Taylor, S. A. and J. L. MacArthur," Digital Pulse Compression Radar Receiver," APL Tech. Digest, March-April 67, pp 2.

55. Temes, C. L.," Side Lobe Suppression in a Range Channel Pulse Compression Radar," IRE Trans. MIL, VOL. MIL-6, Apr. 62, pp 162.

56. Tompkins, D. N., <u>Codes with Zero Correlation</u>, Hughes Aircraft Co., Tech. Memo No. 651, Jun. 60.

57. Turin, G. L.," An Introduction to Matched Filters," IRE Trans. IT, Vol. IT-6, Jun. 60, pp 311.

58. Turyn, R.," On Barker Codes of Even Length," Proc. IEEE, Vol. 51, Sep. 63, pp 1256.

59. Turyn, R., <u>Optimum Codes Study</u>, Sylvania Electron. Systems, Tech. Rept. No. AFCRC-TR-60-111, Jan. 60.

60. Turyn, R.," Ambiguity Functions of Complementary Sequences," IEEE Trans. IT, Vol. IT-9, Jan. 63, pp 46.

61. Turyn, R. and J. Storer," On Binary Sequences," Proc. Amer. Math. Soc., Vol. 12, Jan. 61, pp 394.

62. Welti, G. R.," Quaternary Codes for Pulsed Radar," IRE Trans. IT, Vol. IT-6, Jun. 60, pp 400.

63. White, D. M., <u>Synthesis of Pulse Compression Waveforms with Weighted Finite Frequency Combs</u>, Johns Hopkins Univ., Appl. Phy. Lab. Tech. Memo No. TG-934, Aug. 67.

64. Woodward, P. M., <u>Probability and Information Theory with Applications to Radar</u>, Vol. 3, Pergamon Press, London, 1953.

65. Zierler, N.," Linear Recurring Sequences," J. Soc. Ind. Appl. Math., Mar. 59, pp 31.